Final Report

OPTIMAL COMBINING OF GROUND-BASED SENSORS FOR THE PURPOSE OF VALIDATING SATELLITE-BASED RAINFALL ESTIMATES

by

Witold F. Krajewski

David T. Rexroth

Kiriakie Kiriaki

Sponsored by:
National Aeronautics and Space Administration
Goddard Space Flight Center
Greenbelt, Maryland 20771
(Grant No. NAG 5 1126)

Department of Civil and Environmental Engineering
and
Iowa Institute of Hydraulic Research
The University of Iowa
Iowa City, Iowa 52242

May 1991

cc: NSTIF

ABSTRACT

The study describes two problems related to radar rainfall estimation. The first part is a description of a preliminary data analysis for the purpose of statistical estimation of rainfall from multiple (radar and raingage) sensors. Raingage, radar and joint radar-raingage estimation is described and some results are give. Statistical parameters of rainfall spatial dependence are calculated and discussed in the context of optimal estimation. Quality control of radar data is described also. The second part describes radar scattering by ellipsoidal raindrops. Analytical solution is derived for the Rayleigh scattering regime. Single and volume scattering is presented. Comparison calculations with the known results for spheres and oblate spheroids are shown.

TABLE OF CONTENTS

PART I

ESTIMATION OF RAINFALL FROM RADAR AND RAINGAGES

I.1. INTRODUCTION

Estimation of global rainfall is an important component of global climate studies. This has been well established and documented (Simpson [1989], Thiele [1987], Wilkerson [1988], Arkin and Ardunay [1990]). Due to the fact that over 70% of the Earth's surface is covered by oceans it is necessary to use satellite technology for global rainfall estimation. Satellite methods of rainfall estimation rely on indirect ways of inferring rainfall over an area based on measurements of radiation emmitted from several different frequency bands. For review of satellite methods of rainfall estimation refer to Barrett and Martin [1981], Adler and Negri [1988], or Arkin and Ardunay [1990]. Satellite estimation methods require validation because they are based on indirect inference. Validation simply means comparing the estimation with other independently obtained estimates of the same rainfall. The validation will not be meaningful if the reference methods are of poor quality or if their accuracy cannot be established. The reference methods are typically based on raingage networks and more recently on estimates from weather radars. It is the purpose of this report to discuss these methods with particular emphasis on two aspects:

1. estimation of mean areal rainfall using a combination of radar and raingage observations; and

2. estimation of uncertainty associated with areal estimates of rainfall

A general discussion of the problem will be illustrated with analysis of radar rainfall data from Darwin, Australia. The data set used in the study is fully described in Krajewski and Rexroth [1990].

I.2. RAINGAGE RAINFALL ESTIMATION

Raingages are the most traditional means of measuring rainfall. The observed rainfall represents a point value and in order to make an assessment of areal rainfall one needs to resort to interpolation methods. Mathematically the problem can be defined in the following way. Suppose that the true but unknown mean areal rainfall is

$$R_A = \frac{1}{A} \int_A P(\mathbf{u},t)\,d\mathbf{u} \qquad (1)$$

where A is the area of interest, $\mathbf{u}=(x,y)$ is a two dimensional space location, and P is the true rainfall process. The index t signifies the temporal aspect of the problem. In the

following derivations this index will be dropped to simplify the notation. It will be assumed that both the estimated areal rainfall and its observations are given at the same time scale. The temporal resolution of the data used in this work is either one hour or one day. Therefore, equation (1) denotes, say, daily mean area rainfall. The task at hand is to estimate R_A given n point raingage observations $G_i(\mathbf{u},t)$, $i=1,2,\ldots,n$. A linear estimator of the following form can be proposed

$$\hat{R}_A = \sum_{i=1}^{n} \lambda_i G_i(\mathbf{u},t) \tag{2}$$

It is required that the estimator $\hat{R}_A$ be unbiased and give minimum variance. The unbiasedness condition gives

$$E\left[\sum_{i=1}^{n} \lambda_i G_i(\mathbf{u},t) \right] = E\left[\frac{1}{A} \int_A P(\mathbf{u},t)\, d\mathbf{u} \right] \tag{3}$$

By taking advantage of the linearity of both sides of this condition it can be simplified to

$$\sum_{i=1}^{n} \lambda_i E\left[G_i(\mathbf{u},t) \right] = \frac{1}{A} \int_A E\left[P(\mathbf{u},t)\, d\mathbf{u} \right] \tag{4}$$

Assuming that the mean of the rainfall process P is constant in space and that the observations $G_i(\mathbf{u},t)$ are unbiased, equation (4) can be reduced to

$$\sum_{i=1}^{n} \lambda_i = 1 \tag{5}$$

Minimization of the variance of the estimator is accomplished in the following way. First, the variance of the estimator is written as

$$\begin{aligned}\sigma_{R_A}^2 &= E[(R_A-\hat{R}_A)^2] = E[R_A^2] - 2E[R_A\hat{R}_A] + E[\hat{R}_A^2] \\ &= E[\frac{1}{A^2}\int_A\int_A P(\mathbf{u}_1))P(\mathbf{u}_2)\,d\mathbf{u}_1 d\mathbf{u}_2] \\ &- 2E[\frac{1}{A}\int_A \sum_{i=1}^{n}\lambda_i G_i(\mathbf{u})P(\mathbf{u})\,d\mathbf{u}] \\ &+ E[\sum_{i=1}^{n}\sum_{i=1}^{n}\lambda_i\lambda_j G_i(\mathbf{u})G_j(\mathbf{u})]\end{aligned} \tag{6}$$

Making use of the fact that for the second-order stationary processes

$$\mathrm{cov}(\mathbf{v}) = E[P(\mathbf{u}_1)P(\mathbf{u}_2)] - m^2 = \mathrm{cov}(\mathbf{u}_1-\mathbf{u}_2) \tag{7}$$

where m is the mean of the process, equation (6) can be written as

$$\sigma_{R_A}^2 = \frac{1}{A^2}\int_A\int_A \mathrm{cov}(\mathbf{u}_1-\mathbf{u}_2)\,d\mathbf{u}_1 d\mathbf{u}_2$$

$$- \frac{2}{A}\int_A \sum_{i=1}^{n}\lambda_i \mathrm{cov}(\mathbf{u}-\mathbf{u}_i)\,d\mathbf{u}$$

$$+ \sum_{i=1}^{n} \sum_{i=1}^{n} \lambda_i \lambda_j \mathrm{cov}(\mathbf{u}_i - \mathbf{u}_j) \tag{8}$$

The next step is finding the weights λ_i that will minimize the expression (8) subject to the constraint (5). This could be accomplished using the method of Lagrange multipliers. According to the method an unconstraind optimization problem is solved which minimizes the following function

$$F = \sigma^2_{R_A} + 2\mu \left(\sum_{i=1}^{n} \lambda_i - 1 \right) \tag{9}$$

This leads to the following set of linear equations

$$\frac{\partial F}{\partial \lambda_i} = -\frac{2}{A} \int_A \mathrm{cov}(\mathbf{u} - \mathbf{u}_i)\, d\mathbf{u} + 2 \sum_{j=1}^{n} \lambda_j \mathrm{cov}(\mathbf{u}_i - \mathbf{u}_j) + 2\mu = 0$$

$$\text{for } i = 1, 2, \ldots, n \tag{10}$$

$$\frac{\partial F}{\partial \lambda_i} = \sum_{i=1}^{n} \lambda_i - 1 = 0 \tag{11}$$

The solution of this system yields the optimal set of weights denoted with λ_i^* which when substituted into the variance equation (8) give

$$\sigma^2_{R_A} = \frac{1}{A^2} \int_A \int_A \mathrm{cov}(\mathbf{u}_1 - \mathbf{u}_2)\, d\mathbf{u}_1 d\mathbf{u}_2 - \frac{1}{A} \int_A \sum_{i=1}^{n} \lambda_i^* \mathrm{cov}(\mathbf{u} - \mathbf{u}_i)\, d\mathbf{u} - \mu \tag{12}$$

In order to use the above method one needs to estimate the spatial covariance function of the rainfall process. Of course the true covariance, which appears in all the double integral terms, cannot be inferred from the noisy data and will be substituted by a model obtained by fitting a theoretical covariance function to the data.

There are many functions which could be used as models for covariance. For a discussion of these models and the conditions they have to meet see Journel and Huijbregts [1978]. Before a model is decided on, the empirical (or raw) covariance values need to be inspected. In Figures 1 and 2 the raw correlations (normalized covariances) are shown for all the pairs of raingages for daily and hourly data, respectively. The network of raingages under Darwin radar is composed of 22 raingages (21 were included in the analysis). Their locations and the raingage data are discussed in Krajewski and Rexroth [1990]. It is clear from the Figures that there is not much correlation between the rainfall values recorded at the network gages. There are two possible explanations. The first possibility is the statistical sampling variability. The data used in the analysis cover a rather

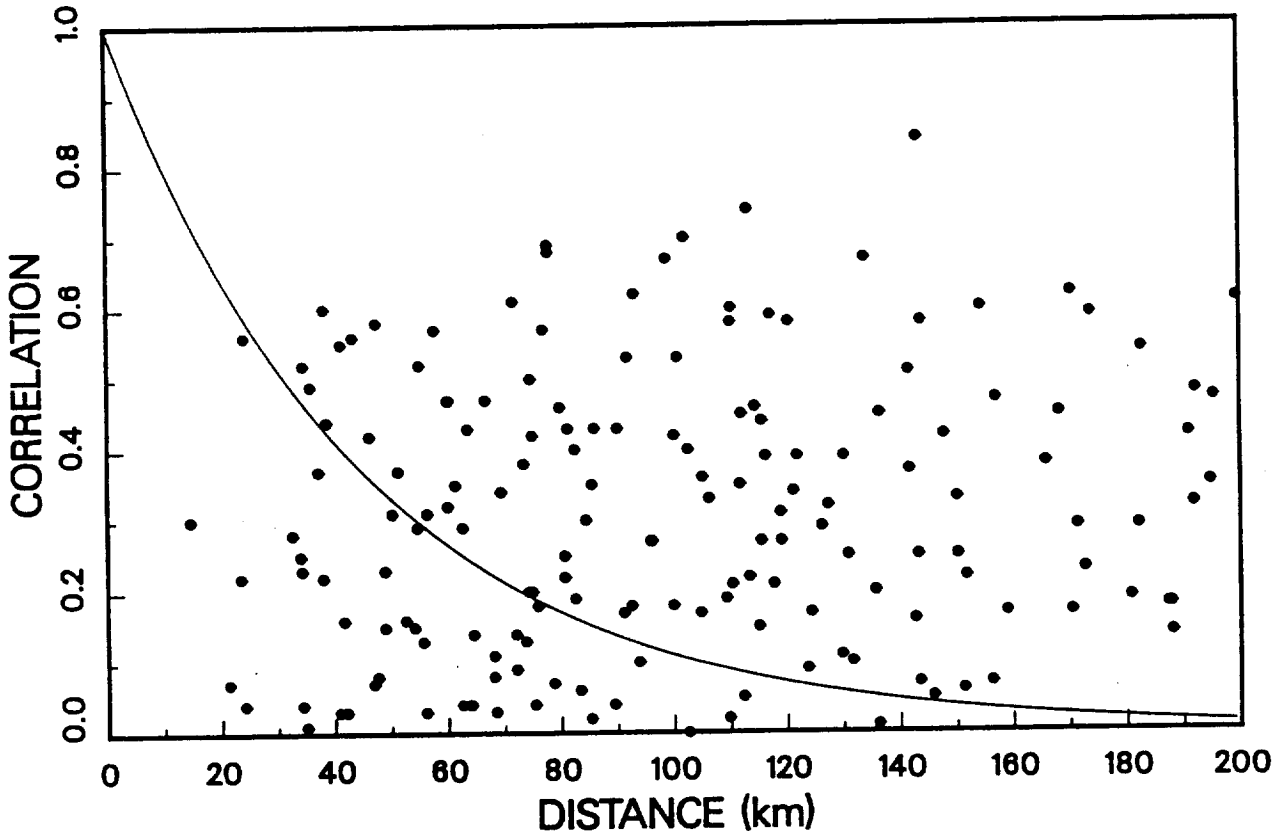

Figure 1. Experimental correlation obtained from daily raingage data for the period December 21, 1987 - January 20, 1988.

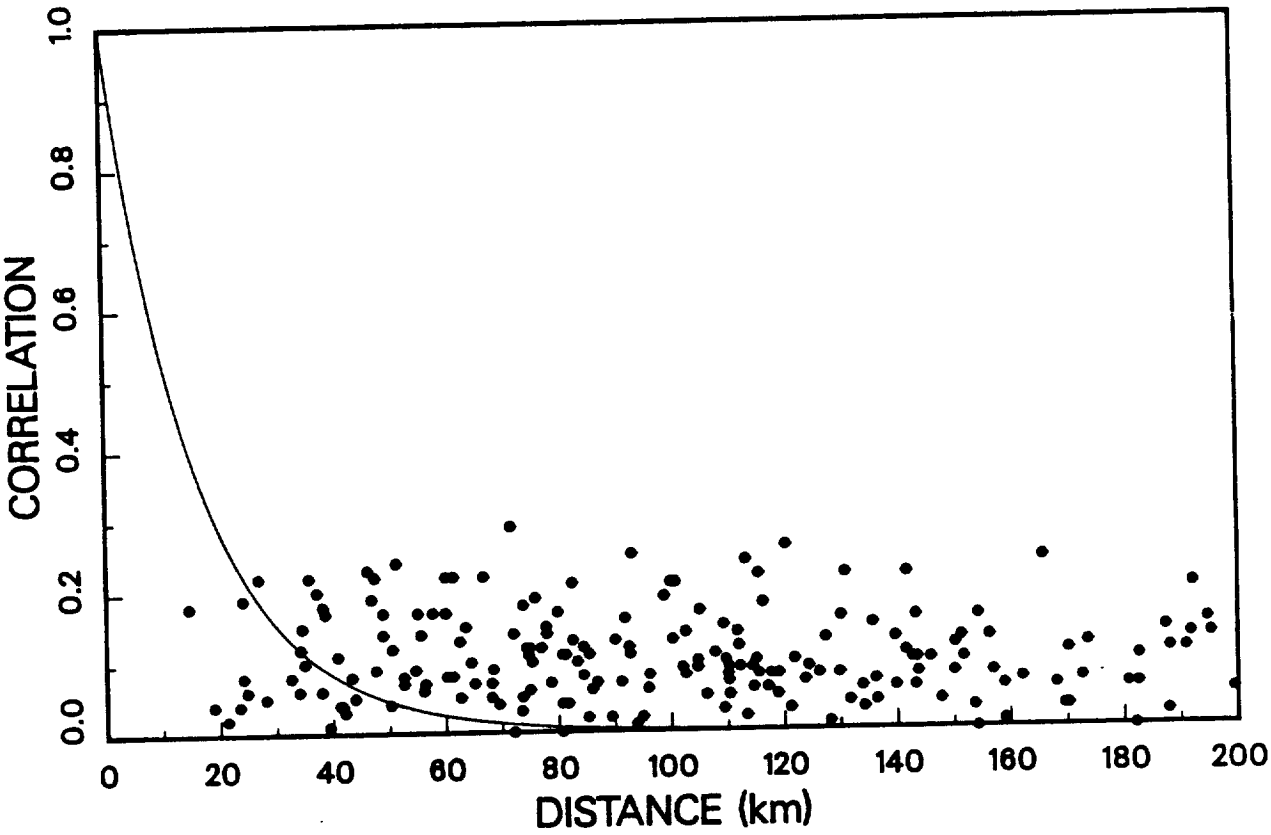

Figure 2. Experimental correlation obtained from hourly raingage data for the period December 21, 1987 - January 20, 1988

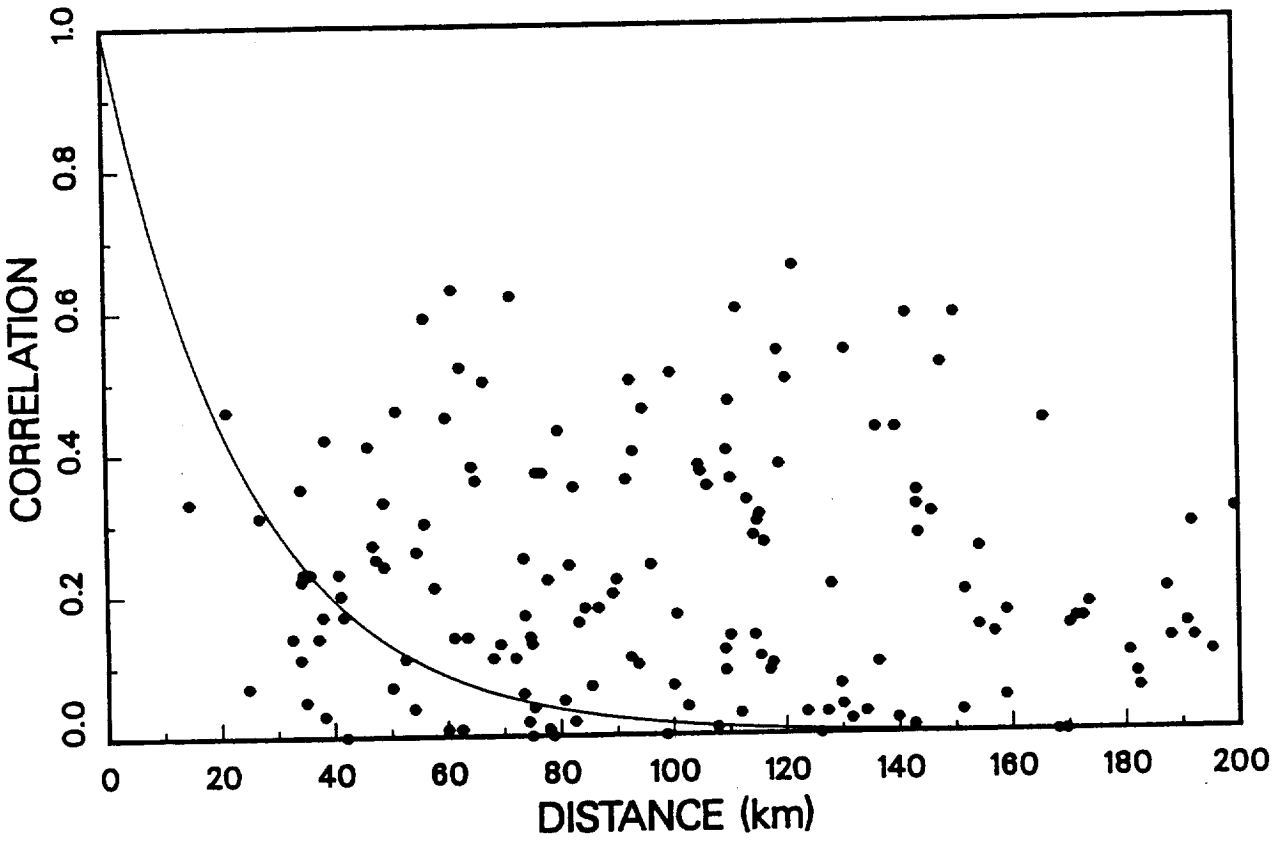

Figure 3. Experimental correlation obtained from daily raingage data for the period October 31, 1987 - May 15, 1988.

short period of time (1 month, December 21, 1987 through January 20, 1988). It is then conceivable that the lack of significant correlation can be attributed to the small sample size used. To verify this hypothesis correlation was calculated for the 6 months of data available covering the period from October 31, 1987 to May 15, 1988. The results are presented in Figure 3. The second possibility is that the existing network is to sparse to capture the fluctuation scale of the events. The shortest distance between any two stations within the network is 14 km and there are only a few pairs of stations separated by a distance less that 30 km. Correlation distance defined as distance at which the exponential correlation drops to 1/e=0.37 depends on the temporal scale of interest. For hourly GATE data the correlation distance is about 20 km (Bell [1987]). For daily GATE data it increases to about 40 km. These numbers represent an overestimation of the point value correlation since they were calculated from radar data averaged in space to 4 by 4 km values. Correlations were also calculated from the Darwin radar-rainfall data. They are shown in Figures 4 and 5. As a conclusion from the above plots and the discussion it is fair to suspect that it is the sparseness of the network that causes the lack of significant correlation. It can be shown that, if there is no significant correlation the weights are all equal and the estimator becomes a simple average.

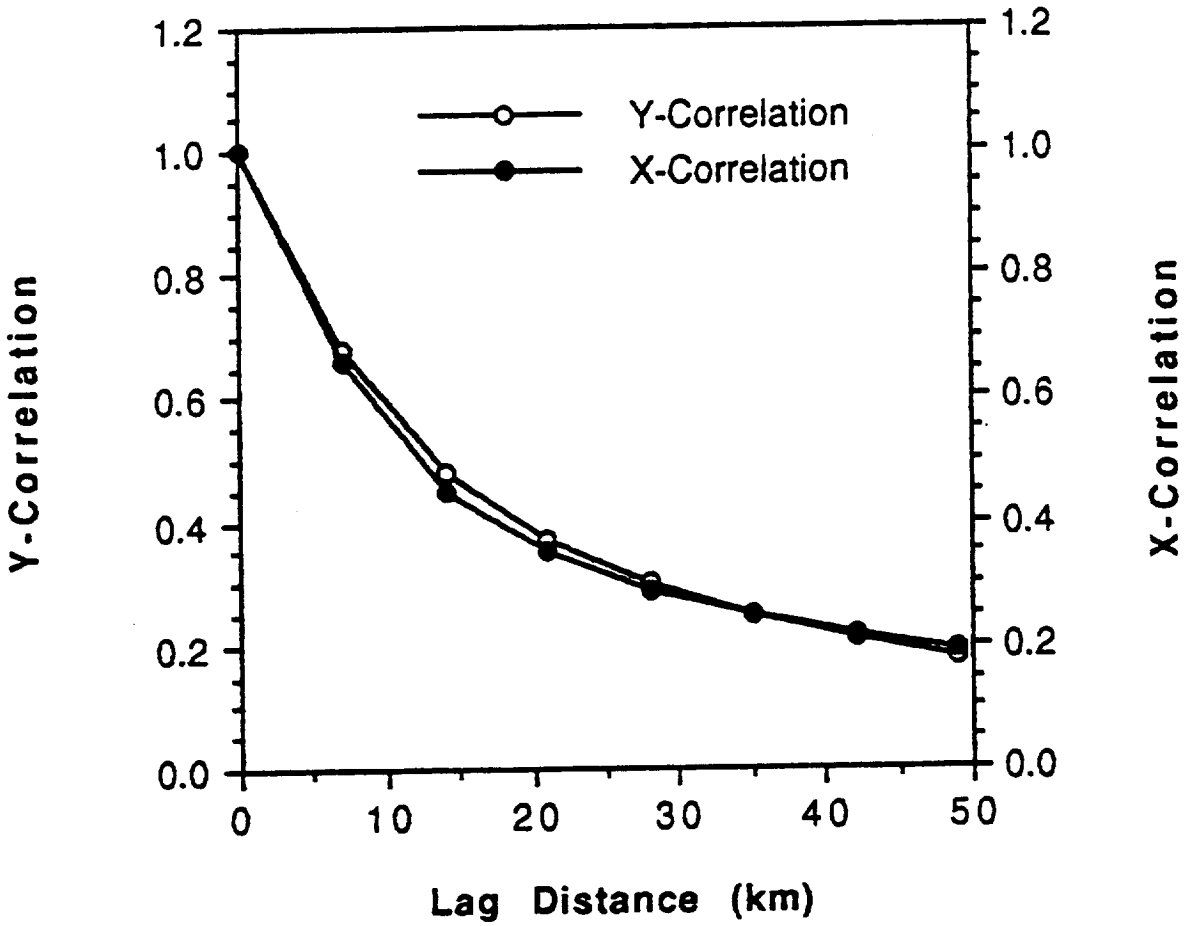

Figure 4. Experimental correlation obtained from hourly radar data for the period December 21, 1987 - January 20, 1988.

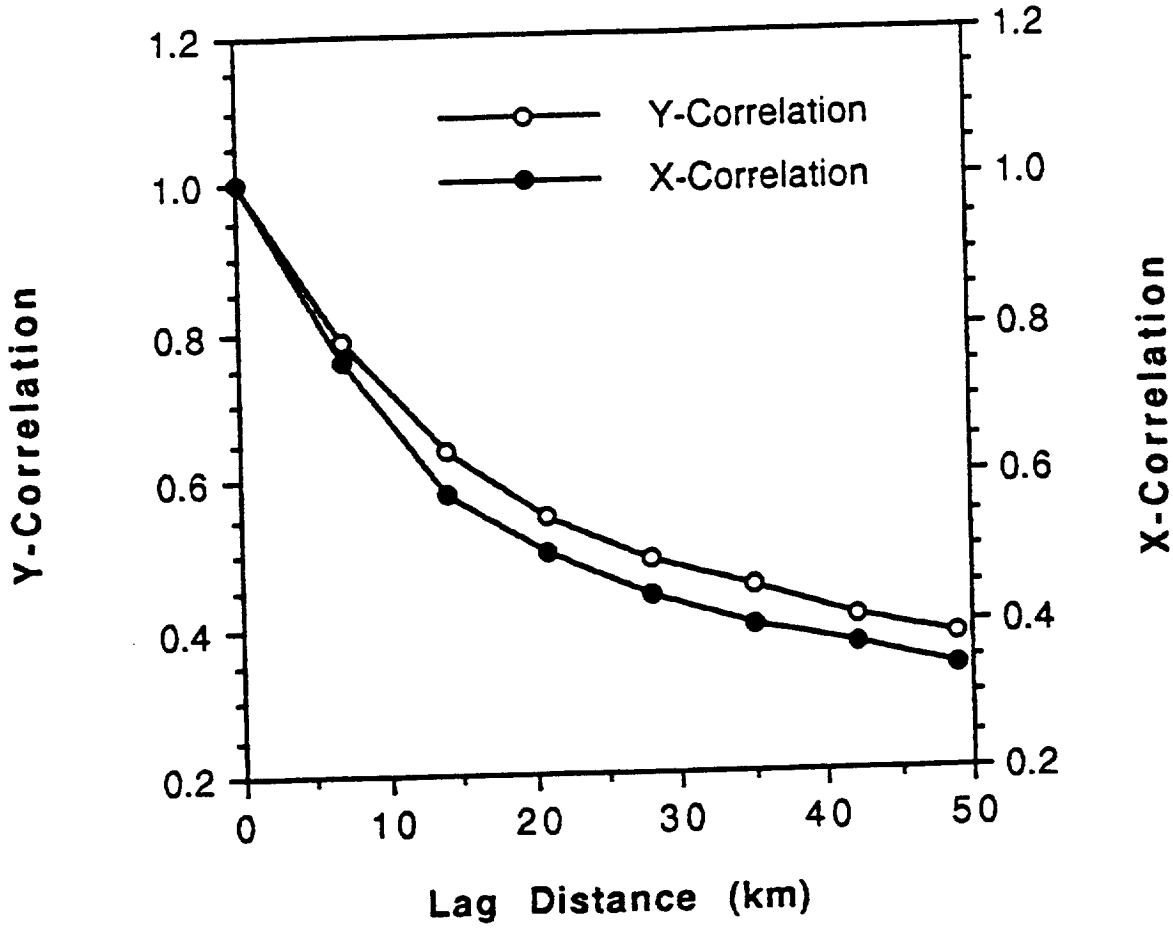

Figure 5. Experimental correlation obtained from daily radar data for the period December 21, 1987 - January 20, 1988.

Based on the raingage data the average monthly rainfall rate for the Darwin radar umbrella, calculated from the raingage data is 0.45 mm/hr. The values of daily rainfall are given in Table 1. The variances of these rainfall estimates can be calculated simply as

$$\mathrm{Var}\{R_A - P\} = 1/n[\sigma^2 - E\{\mathrm{Cov}(\mathbf{X},\mathbf{Y})\}] \qquad (13)$$

where $\mathbf{X},\mathbf{Y}$ are independent uniformly distributed points (gages) in the domain of interest. If this domain is large compared to the effective range of the covariance function the second term in (13) becomes negligible. In our case the domain of interest has radius of 170 km while the effective range of the correlation is only about 20 km. Assuming temporal independence of the daily estimates the standard deviation of the monthly estimate of the average rainfall rate is about 0.02 mm/hr. This corresponds to about 13 mm for monthly rainfall accumulation.

Table 1. Daily Areal Averages of Radar and Gauges

Date	R-Rate (mm/hr)	R-Acum (mm)	G-Rate (mm/hr)	G-Acum (mm)
12/21/87	0.8937	10.7	1.1823	28.4
12/22/87	1.0331	7.2	1.3912	33.4
12/23/87	1.1231	20.2	1.5884	38.1
12/24/87	0.5020	2.0	0.1164	2.8
12/29/87	0.2238	2.5	0.0794	1.9
12/30/87	0.4721	11.3	1.0933	26.2
12/31/87	0.9245	22.2	1.4980	36.0
01/01/88	0.0062	0.1	0.0000	0.0
01/02/88	0.2696	6.5	0.4370	10.5
01/03/88	0.2572	4.4	0.1951	4.7
01/04/88	0.3915	9.4	0.3968	9.5
01/05/88	0.2628	6.3	0.2799	6.7
01/06/88	0.1724	3.3	0.3857	9.3
01/07/88	0.1262	3.0	0.0590	1.4
01/08/88	0.1488	3.6	0.2360	5.7
01/09/88	0.3547	7.1	0.7094	17.0
01/10/88	0.5545	11.6	0.4539	10.9
01/11/88	0.5127	12.3	0.4026	9.7
01/12/88	0.1859	4.5	0.0919	2.2
01/13/88	0.1783	4.3	0.3670	8.8
01/14/88	0.1640	3.6	0.2223	5.3
01/15/88	0.0867	2.1	0.0097	0.2
01/16/88	0.3599	8.6	0.3957	9.5
01/17/88	0.0752	1.8	0.0164	0.4
01/18/88	0.0484	1.2	0.0000	0.0
01/19/88	0.2773	5.8	0.0919	2.2
01/20/88	0.2725	2.5	0.1092	2.6

The monthly areal averages for radar and gages are as follows: R-Rate=0.36 mm/hr, R-Accum=147 mm, G-Rate=0.44 mm/hr, G-Accum= 291 mm. The gage rates were calculated with the assumption of 24 hr measurement by all gages during the entire period. This was not always the case. Missing hours were accounted for in the monthly and daily radar averages. The Channal gage was not included in the gage averages.

I.3. RADAR-RAINFALL ESTIMATION

Estimation of Darwin rainfall based on the radar data was described in Krajewski and Rexroth (1990). In their atlas of radar-rainfall no attempt was made to use the best (in some sense) Z-R relationship or special preprocessing of the radar data. The 1.5 km CAPI data prepared at the NASA Goddard Space Flight Center were used. The Z-R relationship used was the following: a=230 and b=1.25.

It was found that anomalous propagation presented a severe problem and therefore, a manual computer graphics-aided procedure was utilized to eliminated it as much as possible. Also, a quality control procedure aimed at detecting isolated outliers (see Krajewski, 1987) was applied to both hourly and daily rainfall fields converged to a 4 km by 4 km resolution grid. Outliers were defined as those data points which were statistically inconsistent with their immediate neighborhoods. The outliers detected in the daily fields are listed in Table 2. The critical parameter α which appears in the table controls the sensitivity of the method. Low values of the parameter indicate high sensitivity and, as a result, many points are questioned as being outliers. High values of α correspond to lower sensitivity of the method, and as a result some of the "not-so-obvious" outliers may slip through the quality control. Based on the simulation study performed by Krajewski (1987) the optimal choice of the critical param-

eter for daily rainfall fields is α=3.0. The total number of outliers detected with this value of α in the studied period was 8.

Once outliers are detected the problem becomes how to accommodate them. By accommodation is meant replacement of the erroneous values with their surrogates. One "safe" choice of such replacement is to use the local mean of the surrounding data.

After the quality control steps were implemented monthly rainfall based on radar observations was calculated from the daily fields. Comparison of daily and monthly values of radar-rainfall is given in Table 2.

Critical Parameter α															
Date	1.0			2.0			3.0			4.0			5.0		
	I	J	R	I	J	R	I	J	R	I	J	R	I	J	R
12/22/87	74	85	49	88	69	101	88	69	101	88	69	101			
12/22/87	72	87	33	88	70	61									
12/29/87	51	13	31	23	34	69									
12/29/87	20	35	48												
12/31/87				48	31	66	48	31	66	48	31	66			
01/03/88	23	21	28												
01/06/88	11	36	41	11	36	41									
01/06/88	34	38	19												
01/06/88	34	39	15												
01/06/88	71	81	20												
01/07/88	21	41	13												
01/07/88	21	45	34												
01/08/88	89	63	52	73	29	87	73	29	87						
01/09/88	29	14	52												
01/09/88	36	31	54												
01/10/88	50	12	299	26	32	428	26	32	428	23	21	1084	23	21	1084
01/10/88	26	321	428	30	33	287	30	33	287	26	32	428	26	32	428
01/10/88	27	31	189												
01/11/88	63	82	.18												
01/11/88	64	84	.15												
01/12/88	9	56	47	9	56	47									
01/13/88	41	11	40												
01/14/88	59	29	31												
01/15/88	85	26	23	62	83	33				92	59	107			
01/15/88										92	58	148			
01/05/88	62	83	33												
01/16/88	66	39	62												
01/17/88	37	41	31												
01/17/88	62	68	37												

Table 2. List of outliers detected in the daily data.

I.4. RADAR-RAINGAGE COMBINATION

The time-area average of interest can be expressed mathematically according to equation (1). An estimate of R_{TA} denoted $\hat{R}_{TA}$ can be obtained from a number of ground-based sensors. The most appropriate network for the purpose of satellite rainfall validation exercise seems to be a combined network of a radar and a number of raingages. We could write

$$\hat{R}_{TA} = g(\underline{Z}_R, \underline{Z}_G) \tag{14}$$

where $\underline{Z}_R=(Z_{R1}, Z_{R2}, \ldots, Z_{RNR})$ is a vector of NR radar observations within the area of interest A, $\underline{Z}_G=(Z_{G1}, Z_{G2}, \ldots, Z_{GNG})$ is a vector of NG corresponding raingage observations, and g is a function of NG and NR arguments. It is often taken to be linear, however it can also be nonlinear. The error term ε resulting from the approximation (14) is a random component which could be characterized by its mean μ_ε and variance σ^2_ε. Below we outline a methodology to compute $\hat{R}_{TA}$ and the associated σ^2_ε from radar and raingage observations. This methodology is based on the main assumption that rainfall is a realization of a spatial stochastic process (random field).

Weather radars could be classified as indirect rainfall measuring devices in the sense that they measure parameters related to rainfall and not the rainfall itself. Rainfall

rate, and more precisely rainfall volume is, therefore, estimated from those measurable parameters. As such, radar-rainfall estimates are contaminated by errors which have two basic components: 1) measurement error -- error in measuring the parameters related to rainfall; and 2) inference error-- error due to an imperfect model (i.e., relationship) assumed between the measured parameters and rainfall. For example, one of the major errors introduced in inference models is ice contamination. The chances for ice contamination of the radar signal increase with increasing range. Contamination by ice increases reflectivity for the same rainfall, sometimes by several dB. Another very important measurement error that is normally neglected, but of extreme importance is radar calibration error. This is a systematic error unlike many other errors that are random in nature. This calibration error can easily be of the order of couple dB, which results in high errors in rainfall estimates. This radar calibration error can also drift with time, potentially changing with season. Figure 6 demonstrates the behavior of the bias which results from many different sources, not necessarily just the lack of calibration. Appendix C includes a simulation study of a bias model.(Krajewski and Smith, 1991).

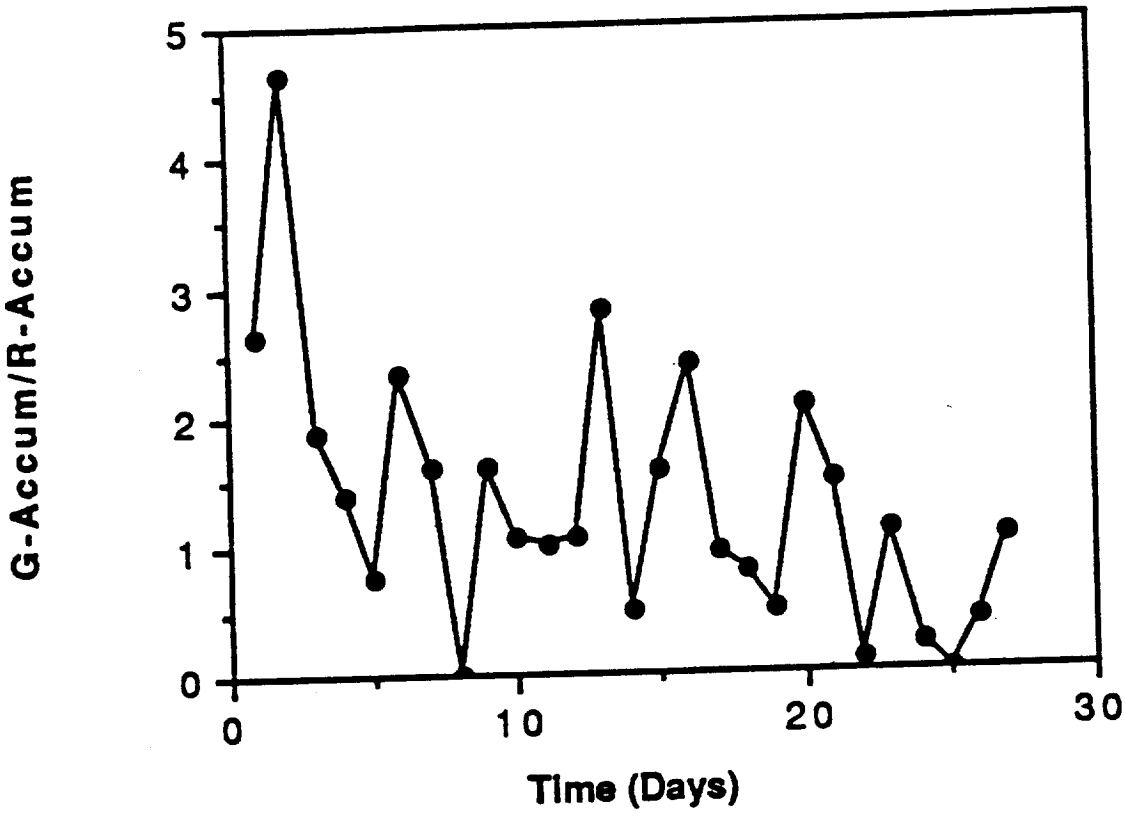

Figure 6. Time series of daily bias of the radar-rainfall. The bias is defined as the ratio of gage to radar mean areal values.

Thus, radars which provide nearly continuous spatial coverage of large areas, are characterized by often significant point errors. On the other hand, a raingage network offers good point accuracy but is characterized by relatively high sampling error related to network density. The premise of a multisensor rainfall estimation is a combination of high spatial resolution of radar and good point accuracy of raingages.

II.4.1 Methodology outline

The characteristics of radar and raingage sensors have been discussed in literature many times (see Wilson and Brandes, [1979]; Doviak and Zrnic, [1984]; Hudlow et al., [1984]; Zawadzki, [1982]; Austin, [1987]; Krajewski, [1987]) justifying the concept of a combined network. Several approaches have been proposed to combine the two types of measurements (Brandes, [1975]; Crawford, [1979]; Eddy, [1979]; Krajewski, [1987]; Seo et al., [1990ab]; Azimi-Zonooz et al., [1988]; Smith et al., [1990]; and Seo and Smith [1990]). The recent works offer a comprehensive approach to the sensor merging problem. This approach is based on the stochastic interpolation technique called cokriging (Journel and Huijbregts, [1978]). Its application requires estimation of spatial covariance functions of data from the involved sensors and the cross-covariance function. The method is capa-

ble of accounting for different sampling geometries of the measurements involved and the measurement error. It is assumed that

$$g(Z_R, Z_G) = \sum_{i=1}^{NR} \beta_{Ri} Z_{Ri} + \sum^{NG} \beta_{Gj} Z_{Gj} \qquad (15)$$

where the coefficients β_{Ri} and β_{Gj} can be found by minimizing the estimation error variance

$$\mathrm{Var}[R_{TA} - \hat{R}_{TA}] = E\{[R_{TA} - \hat{R}_{TA}]^2\} = \sigma_\varepsilon^2 \qquad (16)$$

subject to the condition that we consider only unbiased estimators, i.e.

$$E[\hat{R}_{TA}] = R_{TA} \qquad (17)$$

The solution of this minimization problem is a function of: 1) observations Z_{Ri} and Z_{Gj}; 2) the spatial covariance functions of radar observations and raingage observations; 3) the spatial cross covariance function between the radar and raingage observations; and 4) the spatial covariance functions between the observations and the true rainfall. This last term is of course unknown and in general cannot be estimated from the data. Krajewski [1987] proposed a simple parameterization of this covariance term and performed a limited sensitivity analysis of such an approach. The results showed

quite flat behavior of the criterion function near the optimal location of the parameters. However, the disadvantage of this approach is the lack of meaningful interpretation of the parameters, which in turn may cause difficulties in choosing the parameters for real-data situations. The covariance between the observations and the true rainfall be expressed as a function of measurement error parameters of the two sensors. Radar observations can be expressed as

$$Z_{Ri}=\frac{1}{T}\int_0^T \frac{1}{|S|}\int_S R(t,s)\,dtds+\omega_i \qquad i=1,\ldots,NR \tag{18}$$

where S is the area of a basic radar observation (typically about 4 km x 4 km grid), and ω_i is an error term. This error term can be characterized by its second order moments: the mean and the covariance.

The raingage data represent point observations

$$Z_{Gj}=\frac{1}{T}\int_0^T R(t,s)\,dt + v_j \qquad j=1,\ldots,NG \tag{19}$$

where v_j is a zero mean Gaussian variable with variance σ_v^2 and can be assumed independent of R(t,s). Therefore, the covariance between the observations and the true rainfall can be expressed as a function of μ_ω, cov_ω and σ_v^2. These parameters, in addition to the raingage network density and the

methodology used for combining the two data sets, control the performance of the system.

The precise knowledge of these parameters results in an optimal scheme of merging radar and raingage data. However, in general it is very difficult to obtain the true values of these parameters. Therefore, it is important to investigate the sensitivity of the merging scheme with respect to the uncertainty about the measurement error parameters. Such a sensitivity study can be achieved by a simulation experiment.

It is clear from the previous discussion that the error term of the estimate (14) could be directly used in the validation of the satellite-based rainfall estimation methods.

The problems of estimating the covariance function from a limited sample is demonstrated in Figures 7 and 8 and Table 3. They show the range dependence of the cross-correalation function between the radar and raingage data. A strong effect is evident. The cause was probably the fact that the Darwin radar uses a 5 cm, and therefore attenuating, wavelength.

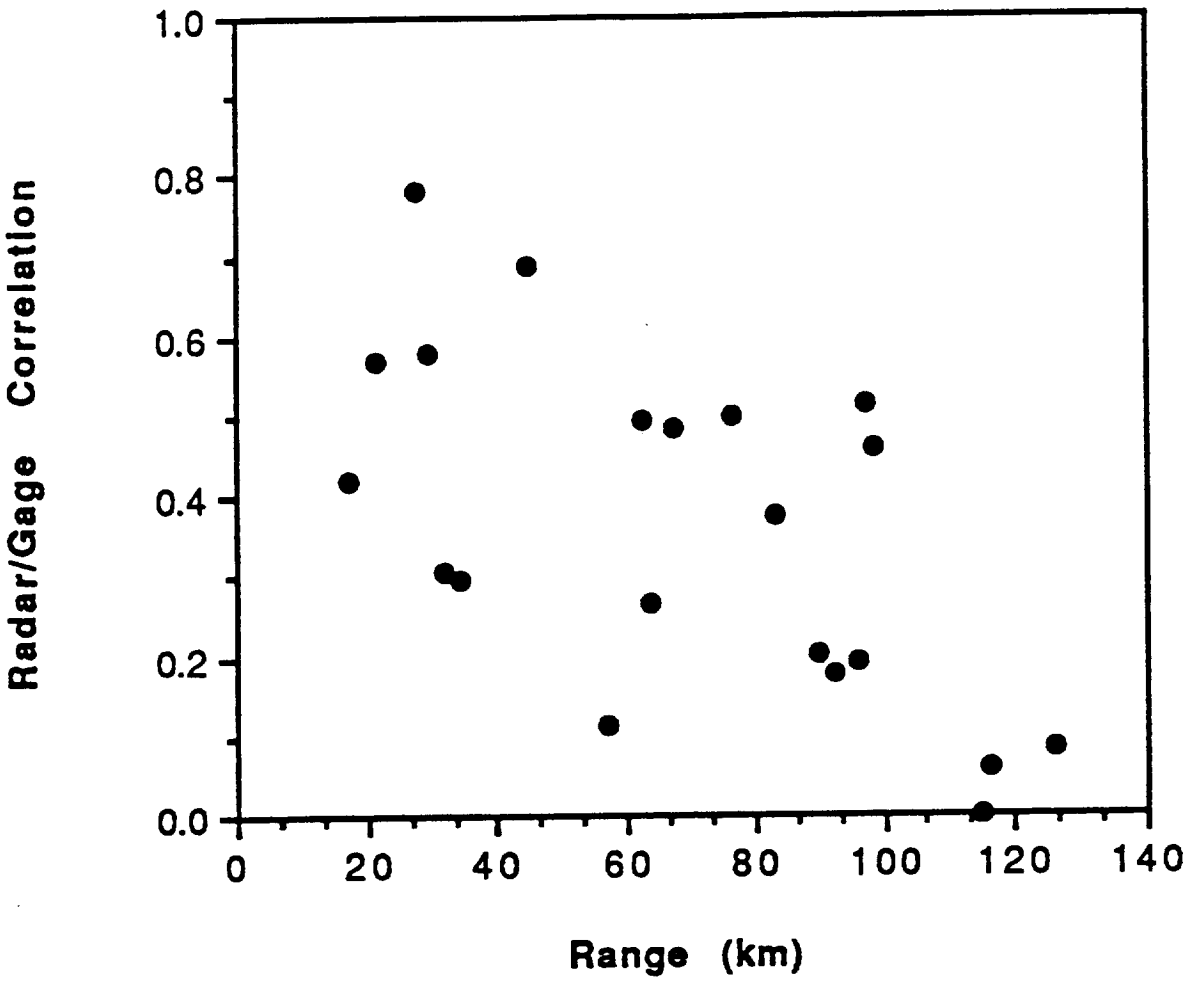

Figure 7. Radar-raingage correlation of hourly data for the co-located points.

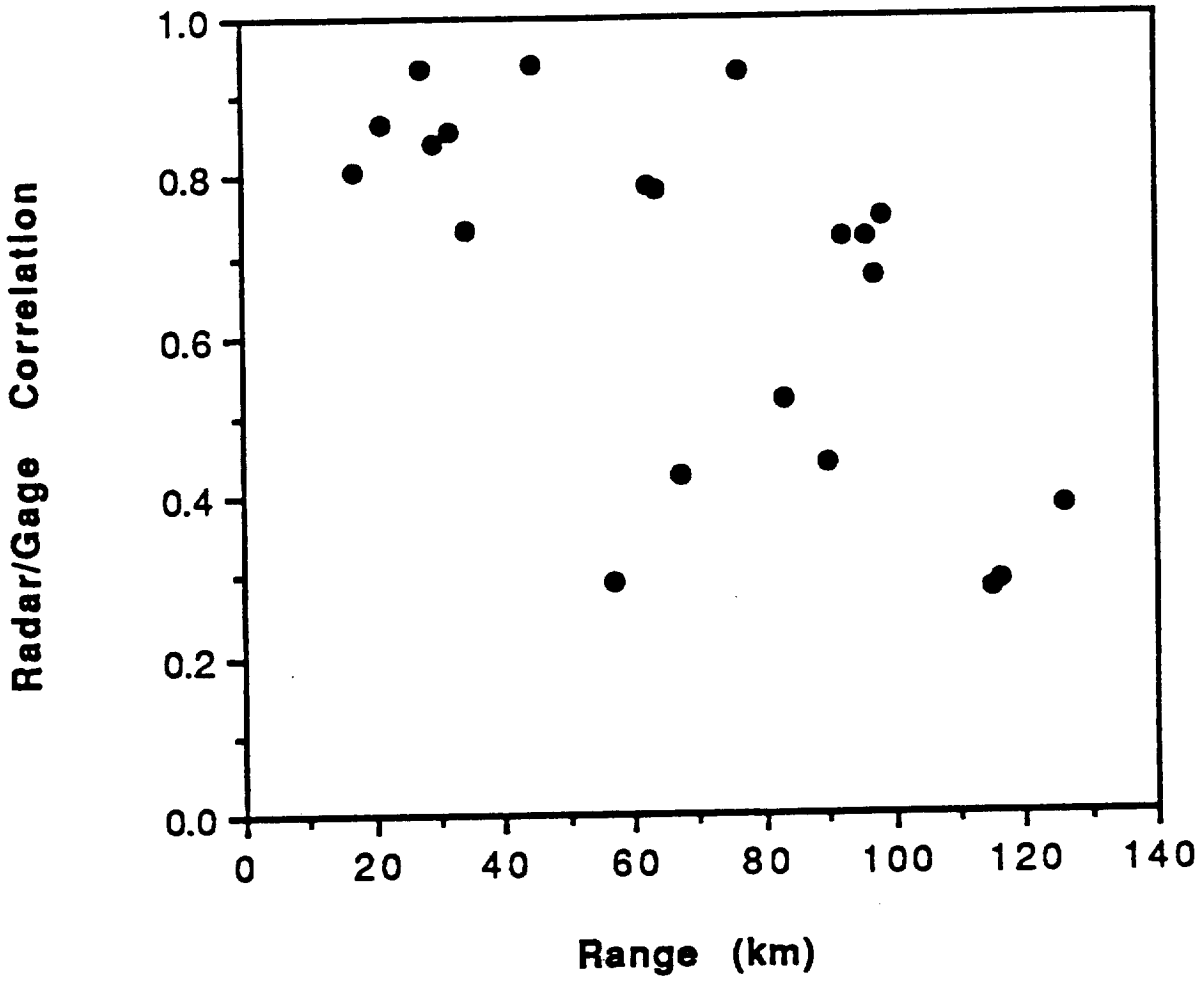

Figure 8. Radar-raingage correlation of daily data for the co-located points.

Table 3. Daily Gage Correlations

Gage #	Gage Name	Range	Correlation	Data Points
1	Annabur	96.25	0.724	23
2	Bachelor	67.27	0.425	22
3	Bathurst Island	83.22	0.521	24
4	Bellville Park	34.13	0.733	23
5	Charles Point	31.58	0.858	24
6	Dum In Mirrie	62.30	0.789	21
7	Garden Point	125.72	0.387	20
8	Goodall Mine	98.27	0.747	19
9	Gunn Point	27.29	0.937	24
10	Humpty Doo	44.78	0.943	25
11	Labelle	29.61	0.842	24
12	Koolpinyah	89.87	0.442	23
13	Litchfield	116.30	0.292	23
14	Mandorah Jetty	17.12	0.807	23
15	McMinns Lagoon	21.47	0.867	25
16	Mt. Bundey	56.82	0.292	26
17	Old Point Stuart	97.51	0.675	23
18	Pickertaramoor	76.16	0.929	22
19	Point Stuart	92.07	0.723	24
20	Snake Bay	114.76	0.282	22
21	Woolner	63.79	0.781	26

It should be evident from the shape of the correlation function that as the separation lag increases the correlation at greater distances from the radar will decrease even faster. Therefore, the radius of the statistical influence of the raingage points on the radar data in the vicinity of the gages is relatively small. It should be expected that the radar-based estimates of rainfall will not be strongly affected by the gage estimates.

I.5. CONCLUSIONS

The performed analysis of the Darwin rainfall data for one monthly period demonstrated that a statistical approach to rainfall estimation using both radar and raingage data is faced with major problems. The two biggest problems seem to be:

1. Quality control and preprocessing of radar data. Efficient anomalous propagation detection and removal is fundamental to the success of any subsequent estimation approach.

2. Sparseness of the raingage network and its configuration. Since the statistical estimation approach relies on the inference of statistical moments from

the observations, the sampling density is a critical issue. The network of 22 approximately evenly distributed gages cannot capture the spatial variability of the convective and monsoonal rainfall. However, the observed difficulty and apparent lack of strong statistical relation between the radar and the raingage data should be investigated further with a longer data set. The way the network configuration comes into play is through its ability to observe the spatial correlation structure of the investigated process. In the case of the Darwin network it seems that the rainfall process has correlation distance on the order of 20 km or less even on the daily scale. The network which has average intergage separation distance greater then that cannot resolve such a scale.

Investigation of the statistical approach as a nonstationary and space-time process should and will continue.

I.6. REFERENCES

Ahnert, P.R., M.D. Hudlow. and E.R. Johnson, D.R. Greene, and M.R. Dias, *Proposed "on-site" precipitation processing system for NEXRAD,* Preprints of the 21st Radar Meteorology Conference, AMS, Boston, Mass., 378-385, 1983.

Ahnert, P.R., Krajewski, W.F. and Johnson, E.R., *Kalman Filter Estimation of Radar-Rainfall Field Bias,* Preprints of the 23rd Radar Meteorology Conference, AMS, Snowmass, Colorado, 1986.

Arkin P. and Ardanuy, P. *Estimation of climatological scale precipitation from space: a review,* J. of Climate, Vol. 2(11), p. 1229-1238, 1989.

Atlas, D. and Thiele, O.W. (Eds.), *Precipitation Measurements from Space,* Workshop Report, NASA, Goddard Space Flight Center, Greenbelt, Maryland, 1981.

Atlas, D., D. Rosenfeld and D. Short, 1990. *The estimation of convective rainfall by area integrals, 1. The theoretical and empirical basis.* J. Geophys. Res., 95, 2153-2160.

Austin, P.M. *Relation Between Measured Radar Reflectivity and Surface Rainfall*, Monthly Weather Review, Vol. 115, 1053-1069, 1987.

Azimi-Zoonoz, A.A., Krajewski, W.F., Seo, D.J. and Bowles, D.S., *Nonlinear Estimation of Rainfall Using Radar and Raingage Data*. Journal of Stochastic Hydrology, 3, pp. 51-67, 1989.

Bell, T.L. *A Space-Time Stochastic Model of Rainfall for Satellite Remote-Sensing Studies*, Journal of Geophysical Research, Vol. 92, No. D8, pp. 9631-9644, 1987.

Bell, T.L., A. Abdullah, R.L. Martin, and G.R. North, *Sampling Errors for Satellite-Derived Tropical Rainfall: Monte Carlo Study Using a Space-Time Stochastic Model*, Journal of Geophysical Research, Vol. 95, No. D3, pp. 2195-2206, 1990.

Brandes, E.A., *Optimizing Rainfall Estimates with the Aid of Radar*, J. Applied Meteorology, 14, 1339-1345, 1975.

Calheiros, R.V., and I.I. Zawadzki, *Reflectivity-rate relationships for radar hydrology in Brazil*, Journal of Clim. and Appl. Meteorology, 26, 118-132, 1987.

Chiu, L.S., *Estimating areal rainfall from rain area, in Tropical Rainfall Measurement*, Ed. J.S. Theon and N. Fugono, Deepak Publishing, Hampton, VA, 1987.

Collier, C.G., *Accuracy of rainfall estimates by radar, Part I: Calibration by telemetering rain gages*, Journal of Hydrology, 83, 207-233, 1986.

Crawford, K.C., *Considerations for the Design of a Hydrologic Data Network Using Multivariate Sensors*, Water Resources Research, 15(6), 1752-1762, 1979.

Doneaud, A.A., S.I. Niscov, D.L. Priegnitz, and P.L. Smith, *The area-time integral as an indicator for convective rain volumes*, Journal of Clim. and Appl. Meteorology, 23, 555-561, 1984.

Doviak, R.J. and Zrnic, D.S., *Doppler Radar and Weather Observations*, Academic Press, 1984.

Eddy, A., *Objective Analysis of Convective Scale Rainfall Using Gages and Radar*, J. Hydrology, 44, 125-134, 1979.

Fredrick, R.H., V. Myers, E. Auciello, *Five- to 60-minute Precipitation Frequency for Eastern and Central U.S.*, NOAA Tech. Memo. NWS HYDRO-35, National Weather Service, NOAA, U.S. Dept. of Commerce, Silver Spring, MD., 36 pp., 1981.

Hudlow, M.D., J.A. Smith, M. Walton, R. Shedd, *NEXRAD - New Era in Hydrometeorology,* Proceedings of the International Symposium on Hydrological Applications of Weather Radar, pp.B1 (1-7), 1989.

Hudlow, M.D., D.R. Greene, P.R. Ahnert, W.F. Krajewski, T.R. Sivaramakrishnan, E.R. Johnson, and M.R. Dias, *Proposed "off-site" precipitation processing system for NEXRAD,* Preprints of the 21st Radar Meteorology Conference, AMS, Boston, Mass., 394-403, 1983

Hudlow, M.D., R. Arkell, V.L. Patterson, P. Pythowany, F. Richards, and S. Geotix, *Calibration and intercomparison of the GATE C-band radars,* NOAA Tech. Rep. EDIS 31, U.S. Department of Commerce, Washington, D.C., 1979.

Hudlow, M.D., R.K. Farnsworth, and P.R. Ahnert, *NEXRAD Technical Requirements for Precipitation Estimation and Accompanying Economic Benefits,* Hydro Tech. Note 4, Office of Hydrology, Nat. Weather Service, NOAA, Silver Spring, Maryland, 1984.

Joss, J. and A. Waldvogel, *Precipitation measurement and hydrology,* Chap. 29A in Radar in Meteorology, ed. D. Atlas, AMS, Boston, 577-606, 1990.

Journel, A.G., and Huijbregts, Ch.J. *Mining Geostatistics*, Academic Press, 1978.

Koistenen, J.R., *The effect of some measurement errors on radar-derived Z-R relationships*, Preprint Volume of the 23rd Conference on Radar Meteorology, JP50-JP53, 1986.

Krajewski, W.F., *Co-Kriging Radar-Rainfall and Raingage Data*, Journal of Geophysical Research, Vol. 92, No. D8, pp. 9571-9580, 1987a.

Krajewski, W. F., *Radar-Rainfall Data Quality Control by the Influence Function Method*, Water Resources Research, Vol. 23, No. 5, pp. 837-844, 1987b.

Krajewski, W.F. and Georgakakos, K.P., *Synthesis of Radar-Rainfall Data*, Water Resources Research, Vol. 21, No. 5, pp. 764-768, 1985.

Krajewski, W.F. and Georgakakos, K.P., *Physically-Based Simulation of Radar-Rainfall Data from a Space-Time Rainfall Model*. Preprints of the 24th Conference on Radar Meteorology, Tallahassee, Florida, 1989.

Krajewski, W.F., *Multisensor Estimation of Climatological Rainfall* IIHR Report, Iowa Institute of Hydraulic Research, The University of Iowa, 1990 (under preparation).

Krajewski, W.F. and D. Rexroth, *Daily Radar-Rainfall Atlas for One Month of Monsoon in Darwin, Australia* IIHR Report, Iowa Institute of Hydraulic Research, The University of Iowa, 1990 (under preparation).

Krajewski, W.F. and J.A. Smith, *Sampling properties of parameter estimators of a space-time rainfall model*, Water Resources Research, 25(9), 2067-2075, 1989.

Krajewski, W.F. and J.A. Smith, *On the Estimation of Climatological Z-R Relationships*, Submitted to Journal of Applied Meteorology 1990.

Larson, L.W. and E.L. Peck, *Accuracy of Precipitation Measurements for Hydrologic Modeling*, Water Resources Research, Vol. 10, No. 4, pp. 857-863, 1974.

Miller, J.R., *A climatological Z-R relationship for convective storms in the northern Great Plains*, Preprints, 15th Conference on Radar Meteorology, Champaign-Urbana, Oct. 1972, AMS, Boston, 153-154, 1972.

Rodriguez-Iturbe, I. and P.S. Eagleson, *Mathematical Models of Rainstorm Events in Space and Time*, Water Resources Research, Vol.23, No. 1, 1987.

Rosenfeld, D., D. Atlas, and D. Short, *The estimation of rainfall by area integrals, Part 2. The Height-Area Rain Threshold (HART) method,* Journal of Geophysical Research, 95, 2161-2176, 1990.

Seo, D.J., Krajewski, W.F., and Bowles, D.S., *Stochastic Interpolation Methods Used for Multiple Sensor Rainfall Estimation, Experimental Design, 1.* Water Resources Research 26(3), pp. 469-478, 1990.

Seo, D.J., Krajewski, W.F., Bowles, D.S., and Azimi-Zonooz, A., *Stochastic Interpolation Methods Used for Multiple Sensor Rainfall Estimation, Results 2.* Water Resources Research 26(4), pp., 1990.

Seo, D.J. and J.A. Smith, *Rainfall estimation using raingages and radar: a Bayesian approach,* Journal of Stochastic Hydrology and Hydraulics, in press.

Severuk, B. *Methods of Correction for Systematic Error in Point Precipitation Measurement for Operational Use,* Oper. Hydrol. Rep. 21, WMO, Geneva, 1982.

Shedd, R., J.A. Smith, and M.Walton, The sectorized hybrid scan strategy for the NEXRAD precipitation processing system, Proceedings of the International Symposium on Hydrological Applications of Weather Radar, pp.D1 (23-29), 1989.

Simpson, J., R.F. Adler, and G. North, *A proposed tropical rainfall measuring mission (TRMM)*, Bulletin of the American Meteorological Society, 69, 278-295, 1988.

Smith, C.J., The reduction of errors caused by bright bands in quantitative rainfall measurements made using radar, J. Atmos. and Ocean. Technol., 3, 129-141, 1986.

Smith, J.A. and A.F. Karr, *Parameter Estimation for a Model of Space-Time Rainfall* Water Resources Research, Vol. 21, No. 8, 1985.

Smith, J.A. and W.F. Krajewski, *Estimation of the mean field bias of radar rainfall estimates*, Journal of Applied Meteorology, in press.

Smith, J.A. and W.F. Krajewski, *Statistical Modeling of Rainfall Using Radar and Raingage Observations*, Water Resources Research, Vol. 23, No. 10, pp. 1893-1900, 1987.

Smith, J.A., R. Shedd, and M. Walton, *Parameter estimation for the NEXRAD Hydrology Sequence*, Preprints, 24 Conference on Radar Meteorology, 259-263, AMS, Boston, 1989.

Smith, J.A., D-J. Seo, and W.F. Krajewski, *Statistical Framework for Real-Time Radar Rainfall Estimation*, Submitted to Water Resources Research, 1990.

Smith, P.L., D. Cain, and A.S. Dennis, *Derivation of an R-Z relationship by computer optimization and its use in measuring daily areal rainfall,* preprints, 16th Conference on Radar Meteorology, AMS, Boston, 461-466, 1975.

Thiele, O.W. (Ed), *On Requirements for a Satellite Mission to Measure Tropical Rainfall,* NASA RP 1183, 1987.

Thiele, O.W. *Validating Space Observations of Rainfall,* Proceedings of International Symposium on Tropical Precipitation Measurements, Tokyo, Japan, 1987.

Waymire, E., V.K. Gupta, and I. Rodriguez-Iturbe, *A Spectral Theory of Rainfall Intensity at the Meso-b Scale.* Water Resources Research, Vol. 20, No. 10, 1453-1465, 1984.

Wilkerson, J. (Ed). *Validation of Satellite Precipitation Measurements for the Global Precipitation Climatology Project,* Proceedings of an International Workshop, Washington, D.C., 1986, World Meteorological Organization, WMO/TD- No 203, 1988.

Wilson, J.W. and Brandes, E.A., *Radar Measurement of Rainfall--A Summary,* Bull. Am. Meteorol. Soc. 60(9), 1048-1058, 1979.

Yoshino, F. and D. Kozeki, Study on-short term forecasting of rainfall using radar raingage, Technical Report, 19 pp., Hydro. Div., Public Works Research Institute, Ministry of Construction, Tokyo, Japan, 1985.

Zawadzki, I. *On Radar-Raingage Comparison*, J. Appl. Meteorol., 14, 1430-1436, 1975.

Zawadzki, I. *The Quantitative Interpretation of Weather Radar Measurements*, Atmos. Ocean, 20, 158-180, 1982.

PART II

RADAR BACKSCATTERING BY ELLIPSOIDAL RAIN DROPS

ANALYTICAL SOLUTIONS FOR RALYLEIGH REGION

II.1. INTRODUCTION

The calculations of scattering of electromagnetic waves are required in many fields such as remote sensing or radiative heat transfer. In particular, investigation of the scattering of radar waves by raindrops and the scattering of light by small chemical and biological particles is of interest in studies related to global climate modeling.

The solution of the electromagnetic scattering problem by spherical objects is well known as the Mie theory (see [11,26,39]) and has been used to a great advantage in many physical applications. However, the problem of scattering by nonspherical bodies often arises. Many techniques have been developed but each has a limited range of applicability that is determined by the size of the scattering object relative to the wavelength of the incident field.

The scattering by objects that are very small compared to the wavelength can be analyzed by Rayleigh approximation. Since Rayleigh's classical paper [35], there have been many studies performed in this area. Let us only mention Kleinman's work [29,30] for general considerations of the low-frequency electromagnetic scattering problems, Jones [25] for the theoretical aspects of the scattering problem, Kleinman and Senior [30] for their investigations on scattering cross-sections, Asvestas and Kleinman [5,6] for the solution of the low-frequency scattering problem by spheroids and disks, Angell and Kleinmann [1] for polarizability tensors,

Stevenson [37,38] for the solution in the case of the ellipsoid, Siegel [36] for work on bodies of revolution, and Darling and Senior [16] for a general consideration of low-frequency scattering by separable and nonseparable bodies.

Objects whose size is of the order of the wavelength of the incident radiation lie in the range commonly called the resonance region. The classical method of solution in the resonance region utilizes the separation of variables technique. Following this approach Asano and Yamamoto [2] have solved the problem for spheroidal particles. Generalization of their results for the case of randomly oriented spheroidal particles is presented in [3,4].

Based on the well-known T-matrix approach, an integral equation method which was introduced by Waterman [4,5], Barber and Yeh [7] have solved the electromagnetic scattering problem by arbitrarily shaped dielectric bodies. A review article for scattering by non-spherical particles is listed for reference [12].

The scattering of microwaves by raindrops is also a scattering problem which was investigated by many researchers. It is clearly related to the problem of investigating and modeling the shape of raindrops (see Pruppacher-Klett [34] for extensive discussion). The results for spherical raindrops and hail particles are given in Battan [8]. For the results which use the spheroidal description of raindrops refer to Doviak and Zrnic [46]. Also, Warner and Hizal [44] have investigated the scattering of microwaves by

spheroidal raindrops based on an integral equation method. Recently Beard and Als [10,13] have proposed a simple model for the electrostatic equilibrium shape of falling raindrops. We also mention Jameson's work [21,22,23] for radar measurements of rainfall and for estimation of raindrop size distribution. A review of the reflectivity technique of measuring rainfall is presented in [42].

In this work the scattering by ellipsoidal raindrops in low-frequencies is examined. At frequencies below 6 GHz (or wavelength λ=5 cm) most of the rain droplet sizes satisfy the condition $k\alpha<<1$ (k is the wave number and α is the characteristic diameter of the scatterer) and therefore Rayleigh scattering is applicable. The approximate upper limit of the characteristic radius of the scatterer is generally taken to be $\alpha = 0.05\lambda$ [20]. At this radius the error of Rayleigh approximation is less than 4% [27]. We assume that the raindrop is an ellipsoid, with semi-axes a_1, a_2, and a_3. Thus, we have to solve an electromagnetic scattering problem in $\Re^3$. Compared to the already existing solutions, we have one more degree of freedom. We assume an arbitrary direction of the incident radiation on the scatterer, and we examine the far-field patterns, taking into account the particle size distribution of the rain drops and their random orientation. All our analytical results are graphically compared to the known results for corresponding spheres and spheroids.

II.2. MATHEMATICAL FORMULATION OF THE PROBLEM

II.2.1. Equations of electrodynamics and the fundamental dyadic solution

We consider the propagation of electromagnetic waves in a medium. As it is well known, the electric field $\mathbf{E}(\mathbf{r},t)$ and the magnetic field $\mathbf{H}(\mathbf{r},t)$ are governed in free charge and current space by the Maxwell's equations

$$\nabla \times \mathbf{E}(\mathbf{r},t) = -\mu \frac{\partial \mathbf{H}(\mathbf{r},t)}{\partial t} \tag{1a}$$

$$\nabla \cdot \mathbf{E}(\mathbf{r},t) = 0 \tag{1b}$$

$$\nabla \times \mathbf{H}(\mathbf{r},t) = -\varepsilon \frac{\partial \mathbf{E}(\mathbf{r},t)}{\partial t} + \sigma \mathbf{E}(\mathbf{r},t) \tag{2a}$$

$$\nabla \cdot \mathbf{H}(\mathbf{r},t) = 0 \tag{2b}$$

where ε is the dielectric constant, μ the permeability and σ the conductivity of the medium.

For a general consideration of the electromagnetic problem we refer to [34,39]. Assuming, without any loss of generality, harmonic time dependence for the electric and the magnetic field, we have

$$\mathbf{E}(\mathbf{r},t) = \mathbf{E}(\mathbf{r}) e^{-i\omega t} \tag{3}$$

$$H(\mathbf{r},t)=\mathbf{H}(\mathbf{r})e^{-i\omega t} \tag{4}$$

where ω is the angular frequency. In what follows, we can suppress the time dependence from all field quantities and then, for steady-state waves the equations corresponding to equations (1) and (2) are

$$\nabla\times\mathbf{E}(\mathbf{r})=i\mu\mathbf{H}(\mathbf{r}) \tag{5a}$$

$$\nabla\cdot\mathbf{E}(\mathbf{r})=0 \tag{5b}$$

$$\nabla\times\mathbf{H}(\mathbf{r})=(-\varepsilon i\omega+\sigma)\mathbf{E}(\mathbf{r}) \tag{6a}$$

$$\nabla\cdot\mathbf{H}(\mathbf{r})=0 \tag{6b}$$

Elimination of the $\mathbf{H}(\mathbf{r})$ field in the equations (5) by substitution of the equations (6) gives us the following equations for the electric field

$$\nabla\times\nabla\times\mathbf{E}(\mathbf{r})-k^2\mathbf{E}(\mathbf{r})=0 \tag{7a}$$

$$\nabla\cdot\mathbf{E}(\mathbf{r})=0 \tag{7b}$$

where k is the complex propagation constant

$$k^2=\omega^2\mu\varepsilon(1 + i\frac{\sigma}{\varepsilon\omega}) \tag{8}$$

In particular for nonconducting media ($\sigma = 0$) k is real and it is expressed in terms of the phase velocity c as

$$k = \omega(\mu\varepsilon)^{-1/2} = \omega/c \tag{9}$$

Similarly, the elimination of the $\mathbf{E}(\mathbf{r})$ field in the equations (6) gives us the equations of the same type as equations (7) for the magnetic field.

The fundamental dyadic solution $\tilde{\Gamma}(\mathbf{r},\mathbf{r}')$ satisfies the equation

$$\nabla\times\nabla\times\tilde{\Gamma}(\mathbf{r},\mathbf{r}')-k^2\tilde{\Gamma}(\mathbf{r},\mathbf{r}')=-4\pi\tilde{\mathbf{I}}\delta(\mathbf{r}-\mathbf{r}') \tag{10}$$

where $\mathbf{r}$ is the position of the observation point, $\mathbf{r}'$is the position of the source point, $\tilde{\mathbf{I}}$ is the identity dyadic, and $\delta(\mathbf{r}-\mathbf{r}')$ is the three-dimensional delta function. After some derivations we conclude that

$$\tilde{\Gamma}(\mathbf{r},\mathbf{r}') = \frac{e^{ik|\mathbf{r}-\mathbf{r}'|}}{k^2|\mathbf{r}-\mathbf{r}'|^3}\left\{k^2(\mathbf{r}-\mathbf{r}')\otimes(\mathbf{r}-\mathbf{r}')\right.$$

$$+ (1-ik|\mathbf{r}-\mathbf{r}'|)\left[\tilde{\mathbf{I}}-3\frac{(\mathbf{r}-\mathbf{r}')\otimes(\mathbf{r}-\mathbf{r}')}{|\mathbf{r}-\mathbf{r}'|^2}\right]$$

$$\left.-\tilde{\mathbf{I}}\frac{e^{ik|\mathbf{r}-\mathbf{r}'|}}{|\mathbf{r}-\mathbf{r}'|}\right\} \tag{11}$$

II.2. FORMULATION OF THE SCATTERING PROBLEM

Let us assume that V_2 is a bounded convex and closed subset of $\Re^3$ having a smooth boundary S. Let V_2 be a dielectric with dielectric constant ε_2 and permeability μ_2 that lies in an infinite, homogeneous isotropic medium V_1 with dielectric constant ε_1 and permeability μ_1. We assume, as previously, harmonic time dependence. An incident plane electric wave $\mathbf{E}^{in}$ propagates in the medium V_1 along the propagation vector $\hat{\mathbf{k}}$. Let the corresponding magnetic wave be $\mathbf{H}^{in}$. The two waves have the form

$$\mathbf{E}^{in}(\mathbf{r}) = \hat{\mathbf{b}} e^{ik_1 \hat{\mathbf{k}}\cdot\mathbf{r}} \tag{12}$$

$$\mathbf{H}^{in}(\mathbf{r}) = \hat{\mathbf{k}}\times\hat{\mathbf{b}}\sqrt{\varepsilon_1/\mu_1}\; e^{ik_1 \hat{\mathbf{k}}\cdot\mathbf{r}} \tag{13}$$

where $\hat{\mathbf{b}}$ is the unit polarization vector for the electric field so that $\hat{\mathbf{b}}\cdot\hat{\mathbf{k}} = 0$ and k_1 is the propagation constant for V_1.

If $\mathbf{E}(\mathbf{r})$, $\mathbf{H}(\mathbf{r})$ are the scattered electric and magnetic waves, respectively, and $\mathbf{E}_i(\mathbf{r})$, $\mathbf{H}_i(\mathbf{r})$ the total fields for the spaces V_i, $i = 1,2$, then due to linearity the total waves are given by the sum of the incident plus the scattered field.

The vector fields $\mathbf{E}^{in}(\mathbf{r})$, $\mathbf{E}(\mathbf{r})$, $\mathbf{E}_i(\mathbf{r})$, $\mathbf{H}^{in}(\mathbf{r})$, $\mathbf{H}(\mathbf{r})$, $\mathbf{H}_i(\mathbf{r})$, satisfy the equations

$$\nabla \times \nabla \times \mathbf{w}(\mathbf{r}) - k_i^2 \mathbf{w}(\mathbf{r}) = 0 \quad \mathbf{r} \in V_i \; i = 1, 2 \tag{14}$$

$$\nabla \cdot \mathbf{w}(\mathbf{r}) = 0 \tag{15}$$

where

$$k_i^2 = \omega^2 \varepsilon_i \mu_i \tag{16}$$

The boundary conditions for the electric field on the surface of the dielectric are given by the equation

$$\hat{\mathbf{n}} \times \mathbf{E}_1(\mathbf{r}') = \hat{\mathbf{n}} \times \mathbf{E}_2(\mathbf{r}') \qquad \mathbf{r}' \in S \tag{16a}$$

$$\hat{\mathbf{n}} \times [\nabla \times \mathbf{E}_1(\mathbf{r}')] = \frac{\mu_1}{\mu_2} \hat{\mathbf{n}} \times [\nabla \times \mathbf{E}_1(\mathbf{r}')] \qquad \mathbf{r}' \in S \tag{16b}$$

On the surface of the scatterer the boundary condition

$$\hat{\mathbf{n}} \cdot \mathbf{E}_1(\mathbf{r}') = \frac{\varepsilon_2}{\varepsilon_1} \hat{\mathbf{n}} \cdot \mathbf{E}_2(\mathbf{r}') \qquad \mathbf{r}' \in S \tag{16c}$$

must also be satisfied as a consequence of the integral relation (see [37])

$$\int_S \hat{\mathbf{n}} \cdot \mathbf{E}(\mathbf{r}') dS(\mathbf{r}') = 0 \tag{16d}$$

The scattered fields $\mathbf{E}(\mathbf{r})$, $\mathbf{H}(\mathbf{r})$ satisfy the radiation condition, due to Sommerfeld [27]:

$$\lim_{r\to\infty} \mathbf{r} \times (\nabla \times \begin{bmatrix}\mathbf{E}(\mathbf{r}) \\ \mathbf{H}(\mathbf{r})\end{bmatrix}) + ik_1 r \begin{bmatrix}\mathbf{E}(\mathbf{r}) \\ \mathbf{H}(\mathbf{r})\end{bmatrix} = 0 \tag{17}$$

uniformly over all directions.

For a general consideration of the electromagnetic scattering problem we also refer to [27] and [43].

The total electric field admits the following integral representation [1]

$$\mathbf{E}_1(\mathbf{r}') = \mathbf{E}^{in}(\mathbf{r}) - \frac{1}{4\pi} \int_{V_2} \Big[\Big(\frac{\varepsilon_2}{\varepsilon_1} - 1\Big) k_1^2 \, \mathbf{E}_2(\mathbf{r}') \cdot \tilde{\Gamma}(\mathbf{r},\mathbf{r}')$$

$$+ \Big(1 - \frac{\mu_1}{\mu_2}\Big) [\nabla \times \mathbf{E}_2(\mathbf{r}')] \nabla_{\mathbf{r}'} \times \tilde{\Gamma}(\mathbf{r},\mathbf{r}') \Big] dU(\mathbf{r}') \tag{18}$$

where the index $\mathbf{r}'$ means differentiation with respect to the variable $\mathbf{r}$. It also has been proved [28] that the normalized spherical scattering amplitude is given by the relation

$$\mathbf{g}(\hat{\mathbf{r}},\hat{\mathbf{k}}) = \frac{-1}{4\pi}(ik_1)^3 \Big[\int_{V_2} \Big(\frac{\varepsilon_2}{\varepsilon_1} - 1\Big) \mathbf{E}_2(\mathbf{r}') e^{-ik_1 \hat{\mathbf{r}}\cdot\mathbf{r}'} dU(\mathbf{r}') \cdot (\tilde{\mathbf{I}} - \hat{\mathbf{r}} \otimes \hat{\mathbf{r}})$$

$$+ k_1^2 \int_{V_2} (1 - \frac{\mu_1}{\mu_2}) \nabla \times \mathbf{E}_2(\mathbf{r}') e^{-ik_1 \hat{\mathbf{r}} \cdot \mathbf{r}'} \, d\mathbf{U}(\mathbf{r}') \cdot \tilde{\mathbf{I}} \times \hat{\mathbf{r}} \qquad (19)$$

where the normalized scattering amplitude is defined by the relation

$$\mathbf{E}(\mathbf{r}) = \mathbf{g}(\hat{\mathbf{r}}, \hat{\mathbf{k}}) \, h(k_1 r) + O(\frac{1}{r^2}) \qquad (20)$$

where $h(k_1 r)$ is the zeroth order spherical Hankel function of the first kind

$$h(k_1 r) = \frac{e^{ik_1 r}}{ik_1 r} \qquad (21)$$

In radar applications, the bistatic radar cross section σ_{bi} and the back-scattering cross-section σ_b are often used. They are related to normalized scattering amplitude through the relations

$$\sigma_{bi} = \frac{4\pi}{k^2} |\mathbf{g}(\hat{\mathbf{r}}, \hat{\mathbf{k}})|^2 \qquad (22)$$

$$\sigma_b = \frac{4\pi}{k^2} |\mathbf{g}(-\hat{\mathbf{k}}, \hat{\mathbf{k}})|^2 \qquad (23)$$

The back-scattering cross section σ_b is also called the radar cross section. We define as scattering cross-section the ratio of the time average rate (over a period) at which energy is scattered by the body, to the corresponding time average

rate at which the energy of the incident wave crosses a unit area normal to the direction of propagation. The scattering cross-section is related to the normalized scattering amplitude via the relation

$$\sigma_b = \frac{1}{k^2} \int_{|\hat{\mathbf{r}}|=1} |\mathbf{g}(-\hat{\mathbf{k}}, \hat{\mathbf{k}})|^2 \, d\Phi(\hat{\mathbf{r}}) \tag{24}$$

II.3. THE PROBLEM IN LOW-FREQUENCIES

It is possibile to work in low-frequencies when $k\alpha \approx 0$ (i.e., $2\pi\alpha/\lambda \approx 0$), where k is the wavenumber, λ is the wavelength and α is the "characteristic dimension" of the scatterer, that is the radius of the smallest sphere that contains the scatterer. In such a case we can use the potential theory and approximate the problem by a sequence of potential problems. The potential theory approximation is also called long wavelength approximation or low-frequency approximation. The solutions of the vector Helmholtz equation considered as functions of the wavenumber are analytic in the neighborhood of zero. Thus, we can expand them in a convergent power series, which we call low-frequency expansion.

For the electric fields $\mathbf{E}_i(\mathbf{r})$ for i=1,2 we have the expansions

$$\mathbf{E}_i(\mathbf{r}) = \sum_{n=0}^{\infty} \frac{(ik_1)^n}{n!} \phi_n^{(i)}(\mathbf{r}) \tag{25}$$

Inserting this expansion into equation (14) and equating equal powers of k, the following sequence of partial differential equations is obtained

$$\nabla \times \nabla \times \phi_n^{(i)}(\mathbf{r}) + n(n-1) m_i \, \phi_{n-2}^{(i)}(\mathbf{r}) = 0$$

$$\nabla \cdot \phi_n^{(i)}(\mathbf{r}) = 0 \qquad \text{for } n=0,1,2,\ldots \tag{26}$$

where

$$m_i = \begin{cases} 1 & \text{for } i=1 \\ \dfrac{\mu_2 \varepsilon_2}{\mu_1 \varepsilon_1} & \text{for } i=2 \end{cases} \tag{27}$$

The boundary conditions could be transformed into the boundary conditions

$$\hat{\mathbf{n}} \times \phi_n^{(1)}(\mathbf{r}') = \hat{\mathbf{n}} \times \phi_n^{(2)}(\mathbf{r}') \qquad \mathbf{r}' \in S \tag{28a}$$

$$\hat{\mathbf{n}} \times [\nabla \times \phi_n^{(1)}(\mathbf{r}')] = \frac{\mu_1}{\mu_2} \hat{\mathbf{n}} \times [\nabla \times \phi_n^{(1)}(\mathbf{r}')] \qquad \mathbf{r}' \in S \tag{28b}$$

$$\hat{\mathbf{n}} \cdot \phi_n^{(1)}(\mathbf{r}') = \frac{\varepsilon_2}{\varepsilon_1} \hat{\mathbf{n}} \cdot \phi_n^{(2)}(\mathbf{r}') \qquad \mathbf{r}' \in S \tag{28c}$$

The incident wave can also be expanded into a convergent power series of k_1 as follows:

$$\mathbf{E}^{in}(\mathbf{r}) = \hat{\mathbf{b}} \sum_{n=0}^{\infty} \frac{(ik_1)^n}{n!} (\hat{\mathbf{k}} \cdot \mathbf{r})^n \tag{29}$$

The fundamental dyadic solution $\tilde{\Gamma}(\mathbf{r},\mathbf{r}')$ has the expansion

$$\tilde{\Gamma}(\mathbf{r},\mathbf{r}') = \hat{\mathbf{b}} \sum_{n=0}^{\infty} \frac{(ik_1)^n}{n!} \tilde{\gamma}_n(\mathbf{r},\mathbf{r}') \tag{30}$$

where

$$\tilde{\gamma}_n(\mathbf{r},\mathbf{r}') = -\frac{|\mathbf{r}-\mathbf{r}'|^{n-1}}{n+2} \left[(n+1)\tilde{\mathbf{I}} - (n-1)\frac{(\mathbf{r}-\mathbf{r}')\otimes(\mathbf{r}-\mathbf{r}')}{|\mathbf{r}-\mathbf{r}'|^2} \right] \tag{31}$$

and the dyadic $\nabla_{\mathbf{r}'} \times \tilde{\Gamma}(\mathbf{r},\mathbf{r}')$ has the expansion

$$\nabla_{\mathbf{r}'} \times \tilde{\Gamma}(\mathbf{r},\mathbf{r}') = \sum_{n=0}^{\infty} \frac{(ik_1)^n}{n!} \tilde{\delta}_n(\mathbf{r},\mathbf{r}') \tag{32}$$

where

$$\tilde{\delta}_n(\mathbf{r},\mathbf{r}') = (n-1)|\mathbf{r}-\mathbf{r}'|^{n-3}(\mathbf{r},\mathbf{r}') \times \tilde{\mathbf{I}} \tag{33}$$

Substituting (25), (29), (30), and (32) into (18) and equating equal powers of k_1 the following integral relations among the coefficients $\phi_0^{(1)}(\mathbf{r}),\ldots,\phi_n^{(1)}(\mathbf{r})$ are obtained

$$\phi_n^{(1)}(\mathbf{r}) = \hat{\mathbf{b}}\cdot(\hat{\mathbf{k}}\cdot\mathbf{r})^n$$

$$+ \frac{1}{4\pi}\sum_{\rho=0}^{n}\int_{V_2}\Big[\Big(\frac{\varepsilon_2}{\varepsilon_1}-1\Big)\rho(\rho-1)\,\phi_{\rho-2}^{(2)}\,\tilde{\gamma}_{n-\rho}(\mathbf{r},\mathbf{r}')$$

$$-\Big(1-\frac{\mu_1}{\mu_2}\Big)\nabla\times\phi_\rho^{(2)}(\mathbf{r}')\cdot\tilde{\gamma}_{n-\rho}(\mathbf{r},\mathbf{r}')\Big]\,dU(\mathbf{r}') \quad (34)$$

In order to derive the low frequency expansion for the scattering amplitude $\mathbf{g}(\hat{\mathbf{r}},\hat{\mathbf{k}})$ we need the expansion

$$e^{ik_1\hat{\mathbf{r}}\cdot\mathbf{r}'} = \sum_{n=0}^{\infty}(-1)^n\frac{(ik_1)^n}{n!}(\hat{\mathbf{r}}\cdot\mathbf{r}')^n \quad (35)$$

Substituting into equation (19) we obtain

$$\mathbf{g}(\hat{\mathbf{r}},\hat{\mathbf{k}}) = -\frac{1}{4\pi}\sum_{n=0}^{\infty}\frac{(ik_1)^{n+3}}{n!}\binom{n}{\rho}\Big(\frac{\varepsilon_2}{\varepsilon_1}-1\Big)$$

$$\int_{V_2}\phi_{n-\rho}^{(2)}(-1)^\rho(\hat{\mathbf{r}}\cdot\mathbf{r}')^\rho\,dU(\mathbf{r}')\cdot(\tilde{\mathbf{I}}-\hat{\mathbf{r}}\otimes\hat{\mathbf{r}})$$

$$- \frac{1}{4\pi} \left(1 - \frac{\mu_1}{\mu_2}\right) \sum_{n=0}^{\infty} \frac{(ik_1)^{n+2}}{n!} \sum_{\rho=0}^{n} \binom{n}{\rho}$$

$$\int_{V_2} \nabla \times \phi_{n-\rho}^{(2)}(\mathbf{r}') \quad (-1)^{\rho} \quad (\hat{\mathbf{r}} \cdot \mathbf{r}')^{\rho} \; dU(\mathbf{r}') \cdot \tilde{\mathbf{I}} \times \hat{\mathbf{r}} \qquad (36)$$

In particular the leading term approximation as $k_1 \to 0$ is

$$\mathbf{g}(\hat{\mathbf{r}}, \hat{\mathbf{k}}) = - \frac{1}{4\pi} (ik_1)^3 \left\{ \int_{V_2} \left(\frac{\varepsilon_2}{\varepsilon_1} - 1\right) \phi_0^{(2)}(\mathbf{r}') dU(\mathbf{r}') \cdot (\tilde{\mathbf{I}} - \hat{\mathbf{r}} \otimes \hat{\mathbf{r}}) \right.$$

$$\left. - \int_{V_2} \left(1 - \frac{\mu_1}{\mu_2}\right) \nabla \times \phi_1^{(2)}(\mathbf{r}') dU(\mathbf{r}') \cdot \tilde{\mathbf{I}} \times \hat{\mathbf{r}} \right\}$$

$$+ O(k_1^4) \qquad (37)$$

The leading term approximation for the scattering cross-section is given by

$$\sigma = - \frac{k_1^4}{6\pi} \left\{ \left(\frac{\varepsilon_2}{\varepsilon_1} - 1\right)^2 \left| \int_{V_2} \nabla \times \phi_0^{(2)}(\mathbf{r}') dU(\mathbf{r}') \right|^2 \right.$$

$$\left. + \left(1 - \frac{\mu_1}{\mu_2}\right)^2 \left| \int_{V_2} \nabla \times \phi_0^{(2)}(\mathbf{r}') dU(\mathbf{r}') \right|^2 \right\} + O(k_1^6) \qquad (38)$$

In low-frequency regions the magnetic field assumes the series expansions:

$$\mathbf{H}_i(\mathbf{r}) = \sum_{n=0}^{\infty} \frac{(ik_1)^n}{n!} \psi_n^{(i)}(\mathbf{r}) \qquad \mathbf{r}\in V_i \qquad i=1,2 \qquad (39)$$

Following the same procedure as for the electric field we can arrive at a similar sequence of potential problems. We also mention the relation between the coefficients of the low-frequency series expansions for the electric and the magnetic fields given by equations (25) and (39), respectively

$$\nabla\times\phi_n^{(i)}(\mathbf{r}) = \left(m_i \frac{\mu_i}{\varepsilon_i}\right)^{1/2} n\, \psi_{n-1}^{(i)}(\mathbf{r}) \quad \mathbf{r}\in V_i \quad i=1,2 \quad (40)$$

In Rayleigh scattering the radiation zone is determined from the relation

$$S = \frac{d^2}{\lambda} \qquad (41)$$

where d is the characteristic diameter and λ is the wavelength. So, we can assume a single scattering process if every scatterer lies in the radiation zone of any other scatterer, that is at low-frequencies a distance equal to a couple of diameters away from the scatterer justifies the applicability of our method.

II.4. LOW-FREQUENCY SCATTERING BY AN ELLIPSOIDAL DIELECTRIC

Let us assume that the triaxial ellipsoid

$$\sum_{i=1}^{3} \frac{x_i^2}{a_i^2} \leq 1 \qquad \text{with} \qquad 0<a_3<a_2<a_1<\infty \tag{42}$$

is the dielectric scatterer. In order to reflect the geometrical peculiarities of the scatterer we introduce the ellipsoidal harmonic functions.

II.4.1. Ellipsoidal harmonic functions

The ellipsoidal harmonic functions as it is well known, form a complete system of eigenfunctions. In what follows, we will give certain definitions about ellipsoidal harmonics. For details about the ellipsoidal harmonics we refer the reader to Hobson [19]. For details about the solution of the Laplace equation we refer to Morse and Feshbach [32] and for tabulated information of all the coordinate systems to the Moore and Spencer handbook [31].

The ellipsoidal coordinates (ρ,μ,ν) are related to the Cartesian coordinates (x_1,x_2,x_3) by

$$x_1 = \frac{\rho\mu\nu}{h_2 h_3} \tag{43a}$$

$$x_2 = \frac{\sqrt{\rho^2-h_3^2}\,\sqrt{\mu^2-h_3^2}\,\sqrt{h_3^2-\nu^2}}{h_1 h_3} \tag{43b}$$

$$x_3 = \frac{\sqrt{\rho^2-h_2^2}\,\sqrt{h_2^2-\mu^2}\,\sqrt{h_2^2-\nu^2}}{h_1 h_2} \tag{43c}$$

where

$$h_1^2 = a_2^2 - a_3^2 \tag{44a}$$

$$h_2^2 = a_1^2 - a_3^2 \tag{44b}$$

$$h_3^2 = a_1^2 - a_2^2 \tag{44c}$$

and

$$0 \le \nu^2 \le h_3^2 \le \mu^2 \le h_2^2 \le \rho^2 < \infty \tag{44d}$$

Separation of variables for the Laplace equation in ellipsoidal coordinates produces the interior ellipsoidal harmonics

$$E_n^m(\rho,\mu,\nu) = E_n^m(\rho)\; E_n^m(\mu)\; E_n^m(\nu) \tag{45}$$

and the exterior ellipsoidal harmonics

$$F_n^m(\rho,\mu,\nu) = F_n^m(\rho)\ E_n^m(\mu)\ E_n^m(\nu) \tag{46}$$

where E_n^m are the Lamé functions of the first kind and

$$F_n^m(\rho) = (2n+1)\ E_n^m(\rho)\ I_n^m(\rho) \tag{47}$$

with

$$I_n^m(\rho) = \int_\rho^\infty \frac{du}{[E_n^m(u)]^2 \sqrt{u^2-h_2^2}\ \sqrt{u^2-h_3^2}} \tag{48}$$

are the Lamé functions of the second kind. The index n specifies the degree of the corresponding ellipsoidal harmonic and takes the value of n = 0,1,2,3,... while m represents the number of independent harmonic functions of degree n and runs through the values m = 1,2,...,2n+1. In the present work we use the interior ellipsoidal harmonics of degree 0,1 and for the sake of completeness we give their exact form, both in ellipsoidal as well as in Cartesian representation:

$$E_0^1(\rho,\mu,\nu) = 1 \tag{49}$$

$$E_1^1(\rho,\mu,\nu) = \rho\mu\nu = x_1 h_2 h_3 \tag{50a}$$

$$E_1^2(\rho,\mu,\nu) = \sqrt{\rho^2-h_3^2}\sqrt{\mu^2-h_3^2}\sqrt{h_3^2-\mu^2} = x_2h_1h_3 \qquad (50b)$$

$$E_1^3(\rho,\mu,\nu) = \sqrt{\rho^2-h_2^2}\sqrt{h_2^2-\mu^2}\sqrt{h_2^2-\nu^2} = x_3h_1h_2 \qquad (50c)$$

The exterior ellipsoidal harmonics of degree 0,1 are given from equation (46) when equations (49)-(50) are used. The Lamé functions of degree 0,1 that appear in the expression (48) for the elliptic integrals $I_n^m(\rho)$ are

$$E_0^1(\rho) = 1$$

$$E_1^m(\rho) = \sqrt{\rho^2-\alpha_1^2+\alpha_m^2} \qquad \text{for } m=1,2,3 \qquad (51)$$

The set

$$\{E_n^m(\mu)\ E_n^m(\nu): \quad n=0,1,2,\ldots \quad m=1,2,\ldots,2n+1\}$$

forms a complete orthogonal set of surface harmonics on the surface of the ellipsoid.

II.4.2. The elliptic integrals

The four elliptic integrals $I_0^1(a_1)$, $I_1^m(a_1)$ for m=1,2,3 given by equation (48) for $\rho=a_1$ are related by the formula

$$\sum_{i=1}^{3} I_1^m(a_1) = \frac{1}{a_1 a_2 a_3} \tag{52}$$

$$\sum_{i=1}^{3} a_n^2 \, I_1^m(a_1) = I_0^1(a_1) \tag{53}$$

For other useful formulas related to elliptic integrals we refer to [17]. In order to express the elliptic integral $I_0^1(a_1)$ to its canonical form we apply some transformations and conclude in notation of elliptic integrals of the first kind that

$$I_0^1(a_1) = -\frac{1}{\sqrt{a_1^2-a_3^2}} \int_0^{\sin\phi_0} \frac{dt}{\sqrt{1-t^2}\,\sqrt{1-t^2\sin^2 a_0}}$$

$$= -\frac{1}{\sqrt{a_1^2-a_3^2}} F(\phi_0, a_0) \tag{54}$$

where

$$\sigma_0 = \sin^{-1}\sqrt{\frac{a_1^2-a_3^2}{a_1^2}} \tag{55a}$$

$$a_0 = \sin^{-1}\sqrt{\frac{a_1^2-a_2^2}{a_1^2-a_3^2}} \tag{55b}$$

For $I_1^1(a_1)$, for example, we take in standard notation of elliptic integrals of the second kind the relations

$$I_0^1(a_1) = \frac{1}{\sqrt[3]{a_1^2-a_3^2}} \frac{1}{\sin^2 a_0} [E(\phi_0,a_0)-F(\phi_0,a_0)] \tag{56}$$

From equations (52-56) we can evaluate $I_1^2(a_1)$ and $I_1^3(a_1)$.

II.4.3. The zeroth order approximation for the electric field

The zeroth order approximation for the electric field is the solution of the boundary value problem

$$\nabla\times\nabla\times\phi_0^{(i)}(\mathbf{r}) = \mathbf{0} \quad \text{for } i=1,2 \tag{57a}$$

$$\nabla\cdot\phi_0^{(i)}(\mathbf{r}) = 0 \quad \text{for } i=1,2 \tag{57b}$$

$$\hat{\mathbf{n}}\times\phi_0^{(1)}(\mathbf{r}') = \hat{\mathbf{n}}\times\phi_0^{(2)}(\mathbf{r}') \quad \mathbf{r}'\in S \tag{57c}$$

$$\hat{\mathbf{n}} \times [\nabla \times \phi_0^{(1)}(\mathbf{r}')] = \frac{\mu_1}{\mu_2} \hat{\mathbf{n}} \times [\nabla \times \phi_0^{(1)}(\mathbf{r}')] \qquad \mathbf{r}' \in S \tag{57d}$$

$$\hat{\mathbf{n}} \cdot \phi_0^{(1)}(\mathbf{r}') = \frac{\varepsilon_2}{\varepsilon_1} \hat{\mathbf{n}} \cdot \phi_0^{(2)}(\mathbf{r}') \qquad \mathbf{r}' \in S \tag{57e}$$

$$\phi_0^{(1)}(\mathbf{r}) = \hat{\mathbf{b}} + O(\frac{1}{r}) \tag{57f}$$

If we use the well-known representation for the electrostatic problem and that a particular solution for the exterior field is equal to $\hat{\mathbf{b}}$, we have

$$\phi_0^{(1)}(\mathbf{r}) = \hat{\mathbf{b}} + \nabla U_0^{(1)}(\mathbf{r}) \tag{58}$$

$$\phi_0^{(2)}(\mathbf{r}) = \nabla U_0^{(2)}(\mathbf{r}) \tag{59}$$

where the scalar potentials for the exterior and the interior fields are given in terms of second and first kind ellipsoidal harmonics as follows:

$$U_0^{(1)}(\mathbf{r}) = a_{00}^{(1)} I_0^1(\rho) + \sum_{m=1}^{3} a_{01}^{(1)} F_1^m(\rho,\mu,\nu) \tag{60a}$$

$$U_0^{(2)}(\mathbf{r}) = \sum_{m=1}^{3} b_{01}^{(2)m} E_1^m(\rho,\mu,\nu) \tag{60b}$$

For the evaluation of $\nabla F_1^m(\rho,\mu,\nu)$ we will use the general form

$$\nabla F_1^m(\rho,\mu,\nu) = (2n+1)\nabla E_1^m(\rho,\mu,\nu) I_0^1(\rho)$$

$$- (2n+1)\frac{\hat{\rho}}{h\rho}\frac{E_n^m(\rho,\mu,\nu)}{[E_n^m(\rho)]^2\sqrt{\rho^2-h_2^2}\sqrt{\rho^2-h_3^2}} \qquad (61)$$

So,

$$\phi_0^{(1)}(\mathbf{r}) = \hat{\mathbf{b}} + 3h_1h_2h_3\sum_{m=1}^{3}\frac{a_{01}^{(1)m}}{hm} I_1^m(\rho)\hat{\mathbf{x}}_m$$

$$- \frac{\hat{\rho}}{\sqrt{\rho^2-\mu^2}\sqrt{\rho^2-\nu^2}}\left[a_{00}^{(1)1} + 3\sum_{m=1}^{3}\frac{a_{01}^{(1)m}}{E_1^m(\rho)} E_1^m(\mu)E_1^m(\nu)\right] \qquad (62)$$

$$\phi_0^{(2)}(\mathbf{r}) = h_1h_2h_3\sum_{m=1}^{3}\frac{b_{01}^{(2)m}}{hm}\hat{\mathbf{x}}_m \qquad (63)$$

Applying the boundary conditions on $\rho = a_1$ (the surface of the ellipsoid) and by the orthogonality of the surface ellipsoidal harmonics we obtain a system from which we can evaluate the unknown coefficients $a_{00}^{(1)1}$ and $a_{01}^{(i)m}$ for i=1,2.

So, the zeroth order coefficients for the electric field are:

$$\phi_0^{(1)}(\mathbf{r}) = \hat{\mathbf{b}} - \sum_{m=1}^{3} \left[\frac{b_m h_m}{3h_1h_2h_3} \frac{a_1a_2a_3 \left(\frac{\varepsilon_2}{\varepsilon_1} - 1\right)}{a_1a_2a_3 \left(\frac{\varepsilon_2}{\varepsilon_1} - 1\right) I_1^m(a_1) + 1} \right.$$

$$\left. \nabla F_1^m(\rho,\mu,\nu) \right] \tag{64}$$

$$\phi_0^{(2)}(\mathbf{r}) = \sum_{m=1}^{3} \left[\frac{b_m h_m}{h_1h_2h_3} \frac{1}{a_1a_2a_3 \left(\frac{\varepsilon_2}{\varepsilon_1} - 1\right) I_1^m(a_1) + 1} \right.$$

$$\left. \nabla E_1^m(\rho,\mu,\nu) \right] \tag{65}$$

II.4.4. The zeroth order approximation for the magnetic field

The zeroth order approximation for the magnetic field is the solution of a boundary value problem similar to that described by equation (57). This is due to the invariance of the boundary conditions for the dielectric under the substitution $\varepsilon \leftrightarrow \mu$. So, the zeroth order coefficients for the magnetic field are:

$$\psi_0^{(1)}(\mathbf{r}) = \hat{\mathbf{k}}\times\hat{\mathbf{b}} \sqrt{\varepsilon_1/\mu_1} - \sum_{m=1}^{3} \left[\frac{(\hat{\mathbf{k}}\times\hat{\mathbf{b}}) \cdot \hat{\mathbf{x}} h_m \sqrt{\varepsilon_1/\mu_1}}{h_1h_2h_3} \right.$$

$$\frac{a_1 a_2 a_3 \left(\frac{\mu_2}{\mu_1} - 1\right)}{a_1 a_2 a_3 \left(\frac{\mu_2}{\mu_1} - 1\right) I_1^m(a_1) + 1} \nabla F_1^m(\rho,\mu,\nu) \Big] \qquad (66)$$

$$\psi_0^{(2)}(\mathbf{r}) = \sum_{m=1}^{3} \Big[\frac{(\hat{\mathbf{k}}\times\hat{\mathbf{b}})\cdot\hat{\mathbf{x}} h_m \sqrt{\varepsilon_1/\mu_1}}{h_1 h_2 h_3}$$

$$\frac{1}{a_1 a_2 a_3 \left(\frac{\varepsilon_2}{\varepsilon_1} - 1\right) I_1^m(a_1) + 1} \nabla E_1^m(\rho,\mu,\nu) \Big] \qquad (67)$$

II.4.5. The leading term approximation for the normalized scattering amplitude

In order to evaluate the leading term approximation for the normalized scattering amplitude, given by Equation (37) we have to evaluate the integrals which appear in that equation. First, we exploit the relation between the electric and the magnetic low-frequency coefficients given by Equation (40). We have

$$\nabla\times\phi_1^{(2)}(\mathbf{r}) = \frac{\mu_2}{\sqrt{\mu_1\varepsilon_1}} \psi_0^{(2)}(\mathbf{r}) \qquad (68)$$

From the zeroth order approximation for the electric and magnetic fields we obtain

$$\int_{V_2} \phi_0^{(2)}(\mathbf{r}')\,dU(\mathbf{r}') = \frac{4\pi}{3} a_1a_2a_3 \sum_{m=1}^{3} b_m\hat{\mathbf{x}}_m$$

$$\frac{1}{a_1a_2a_3\left(\frac{\varepsilon_2}{\varepsilon_1} - 1\right) I_1^m(a_1)+1} \tag{69}$$

$$\int_{V_2} \nabla\times\phi_1^{(2)}(\mathbf{r}')\,dU(\mathbf{r}') = \frac{4\pi}{3} a_1a_2a_3 \frac{\mu_2}{\mu_1} \sum_{m=1}^{3} (\hat{\mathbf{k}}\times\hat{\mathbf{b}})\cdot\hat{\mathbf{x}}_m$$

$$\frac{1}{a_1a_2a_3\left(\frac{\mu_2}{\mu_1} - 1\right) I_1^m(a_1)+1} \tag{70}$$

The normalized scattering amplitude is given by the relation

$$\mathbf{g}(\hat{\mathbf{r}},\hat{\mathbf{k}}) = -(ik_1)^3 \frac{a_1a_2a_3}{3} \sum_{m=1}^{3} \hat{\mathbf{x}}_m \left[\left(\frac{\varepsilon_2}{\varepsilon_1} - 1\right) \right.$$

$$\left. \frac{b_m}{a_1a_2a_3\left(\frac{\varepsilon_2}{\varepsilon_1} - 1\right) I_1^m(a_1)+1} (\tilde{\mathbf{I}}-\hat{\mathbf{r}}\otimes\hat{\mathbf{r}}) \right.$$

$$+ \left(1 - \frac{\mu_2}{\mu_1}\right) \quad (\hat{k}\times\hat{b})\cdot\hat{x}_m \frac{1}{a_1a_2a_3\left(\frac{\mu_2}{\mu_1} - 1\right) I_1^m(a_1)+1}$$

$$\hat{I}\times\hat{r}\Big] + O(k_1^4) \tag{71}$$

II.4.6. The leading term approximation for the scattering cross-section

For the scattering cross-section the following can be obtained

$$\sigma_s = \frac{8\pi(k_1)^4}{27}\left\{\left(\frac{\varepsilon_2}{\varepsilon_1} - 1\right)^2 a_1^2a_2^2a_3^2\right.$$

$$\sum_{m=1}^{3} \frac{b_m^2}{\left[a_1a_2a_3\left(\frac{\varepsilon_2}{\varepsilon_1} - 1\right) I_1^m(a_1)+1\right]^2}$$

$$+ \left(1 - \frac{\mu_2}{\mu_1}\right)^2 a_1^2a_2^2a_3^2 \sum_{m=1}^{3} \left[(\hat{k}\times\hat{b})\cdot\hat{x}_m\right]^2$$

$$\left.\frac{1}{\left[a_1a_2a_3\left(\frac{\mu_2}{\mu_1} - 1\right) I_1^m(a_1)+1\right]^2}\right\} + O(k_1^6) \tag{72}$$

II.4.7. The back-scattering cross-section

Substituting in Equation (23) we conclude that the leading term approximation for the radar cross-section is given by the relation

$$\sigma_b = \frac{8\pi(k_1)^4}{9} a_1^2 a_2^2 a_3^2 \sum_{m=1}^{3} \left| A_m - k_m \mathbf{A}\cdot\hat{\mathbf{k}}^T + \mathbf{B}\times\hat{\mathbf{k}} \right|^2 + O(k_1^6) \tag{73}$$

where

$$\mathbf{A} = (A_1, A_2, A_3) \quad \text{and} \quad \mathbf{B} = (B_1, B_2, B_3) \tag{74}$$

$$A_m = \left(\frac{\varepsilon_2}{\varepsilon_1} - 1\right) \frac{b_m}{a_1 a_2 a_3 \left(\frac{\varepsilon_2}{\varepsilon_1} - 1\right) I_1^m(a_1) + 1} \tag{75}$$

$$B_m = \left(\frac{\mu_2}{\mu_1} - 1\right) (\hat{\mathbf{k}}\times\hat{\mathbf{b}})\cdot\hat{\mathbf{x}}_m \frac{1}{a_1 a_2 a_3 \left(\frac{\mu_2}{\mu_1} - 1\right) I_1^m(a_1) + 1} \tag{76}$$

Two cases which are of special interest are examined in the sequel. The first is the radar scattering cross-section with vertical polarization, that means

$$\hat{\mathbf{b}}\cdot\hat{\mathbf{x}}_3 = 0 \tag{77}$$

and the second case of the horizontal polarization is

$$(\hat{\mathbf{k}}\times\hat{\mathbf{b}})\cdot\hat{\mathbf{x}}_3 = 0 \tag{78}$$

In these cases the leading term of the backscattering cross-section is also given by Equation (73), but for the vertical polarization we have

$$A_3 = 0 \tag{79}$$

and for the horizontal polarization we conclude from Equation (78) that

$$B_3 = 0 \tag{80}$$

II.5. PARTICLE SIZE DISTRIBUTION

Up to this point we have examined the scattering by a single ellipsoid. However, our main interest lies in how a wave interacts with many randomly distributed particles. The particles we deal with in practice are not usually all one size but normally their sizes are distributed over a certain range. It is, therefore, important to take into account the size distribution of the particles.

Let $n(D)dD$ be the number of particles per unit volume having a dimension (such as diameter) between D and D+dD. The total number of particles per unit volume is then

$$\rho = \int_0^\infty n(d)\,dD \tag{81}$$

which is called number density (or simply density).

We can also define by w(D) a probability density function for finding the particle size between D and D+dD

$$w(D) = \frac{n(D)}{\rho} \tag{82}$$

where

$$\int_0^\infty w(d)\,dD = 1 \tag{83}$$

Now we can define the average cross-section and the average radar cross-section as the following

$$E\{\sigma\} = \int_0^\infty \sigma(D)\,w(d)\,dD \tag{84}$$

and

$$E\{\sigma_b\} = \int_0^\infty \sigma_b(D)\,w(d)\,dD \tag{85}$$

where E{} is the expectation operator and σ, σ_b are given by Equations (72) and (73), respectively. These quantities can be expressed in terms of the semi-axis of the ellipsoid a_1, a_2, and a_3.

The size distribution n(D) in Equation (81) can be represented by an exponential distribution or by a three parameter gamma distribution.

In order to take into account the particle size distribution, using equations (84) and (85), we need to establish a relation between the semi-axes of the ellipsoid (in terms of which are expressed the scattering cross-section and the radar cross-section) and the radius of an equivalent volume spherical raindrop, because in terms of this parameter we have the information on the particle size distribution.

The principal curvatures of a point on the surface of an ellipsoid $\rho=a_1$ are given by the relations

$$k_1 = \frac{a_1 a_2 a_3}{\sqrt{a_1^2-\mu^2}\,\sqrt{a_1^2-\nu^2}}\,\frac{1}{a_1^2-\mu^2} \tag{86}$$

$$k_2 = \frac{a_1 a_2 a_3}{\sqrt{a_1^2-\mu^2}\,\sqrt{a_1^2-\nu^2}}\,\frac{1}{a_1^2-\nu^2} \tag{87}$$

The sum of the principal curvatures at the points on the equator of the ellipsoid are given by the form

$$k_1 + k_2 = a_1^2 a_2 [a_1^2 (a_1^2 + a_3^2) + (a_2^2 - a_1^2) x_1^2]$$
$$\{ a_3^{-2} [a_1^2 + (a_2^2 - a_1^2) x_1^2]^{-3/2} \} \qquad (88)$$

For an oblate spheroid $a_1 = a_2$ and

$$k_1 + k_2 = \frac{a_1}{a_3^2} + \frac{1}{a_2} \qquad (89)$$

which is the same result as in the Appendix of [18]. For $x_1 = 0$ i.e. at the point $(0,a_2,0)$ we have

$$k_1 + k_2 = a_2 \left(\frac{1}{a_3^2} + \frac{1}{a_1^2}\right) \qquad (90)$$

and for $x_1 = a_1$ (the same as for $x_1 = - a_1$), that is at the point $(a_1,0,0)$, we obtain

$$k_1 + k_2 = a_1 \left(\frac{1}{a_3^2} + \frac{1}{a_2^2}\right) \qquad (91)$$

It holds that

$$a_2 \left(\frac{1}{a_3^2} + \frac{1}{a_1^2}\right) \leq k_1 + k_2 \leq a_1 \left(\frac{1}{a_3^2} + \frac{1}{a_2^2}\right) \qquad (91)$$

If we assume that

$$\frac{a_2}{a_1} = \lambda \tag{92}$$

where parameter $\lambda \in (0,1)$, we can study the influence of deformation of the spheroid along the x_2-axis.

We will follow the simplified analysis of the raindrop shape problem due to Green [18]. From the mechanical equilibrium condition on the surface of the drop we have

$$\sigma\left(\frac{1}{R_1} + \frac{1}{R_2}\right) = P_i - P_e \tag{93}$$

where R_1, R_2 are the principal radii of curvature, and P_i and P_e are internal and external pressures, respectively.

By ignoring the aerodynamic and hydrodynamic pressures at the equator of the spheroid Green [18] established the following relation

$$\sigma\left(\frac{1}{R_1} + \frac{1}{R_2}\right) = 2\sigma a_0^{-1} + pg'b = \sigma(ab^{-2} + a^{-1}) \tag{94}$$

where a_0 is the radius of the sphere with equal volume as the oblate spheroid with axes $a_1=a_2=a$, and $b=a_3$. The right hand side of Equation (94) is constant and independent of the point on the equator of the spheroid due to the fact that the equator is a circle. At the points of the equator of the ellipsoid the sum

$$\frac{1}{R_1} + \frac{1}{R_2} = k_1 + k_2 \tag{95}$$

which is obvious from Equation (91) and depends on the specific point. Therefore, in order to establish a relation between the semi-axes a_1, a_2, a_3 and the radius of the equivolume sphere based on the physics of the problem, we first choose the "mean-value" of the sum of curvatures

$$\frac{1}{2}\left[(k_1 + k_2) \Big|_{(a_1,0,0)} + (k_1 + k_2) \Big|_{(0,a_2,0)} \right] =$$

$$\left[a_1^2 a_2^2 (a_1 + a_2) + a_3^2 (a_1^3 + a_2^3) \right] (2a_1^2 a_2^2 a_3^2)^{-1} \tag{96}$$

Now we can establish the equality of the volumes of the ellipsoid and the sphere, through the relation

$$a_1 a_2 a_3 = a_0^3 \tag{97}$$

So, with the same arguments as Green we conclude that

$$a_0 \left[a_1^2 a_2^2 (a_1 + a_2) + a_3^2 (a_1^3 + a_2^3) \right] (2a_1^2 a_2^2 a_3^2)^{-1} = 2 + B\frac{a_3}{a_0} \tag{98}$$

where

$$B = pg' a_0^2 \sigma^{-1} \tag{99}$$

is the Bond number.

If we introduce a new variable

$$\delta = \left(\frac{a_3}{a_0}\right)^2 - 1 \tag{100}$$

we have that

$$a_1 = a_0\sqrt{(1 + \delta)} \tag{101}$$

$$a_2 = \lambda a_0\sqrt{(1 + \delta)} \tag{102}$$

$$a_3 = \lambda^{-1}a_0\sqrt{(1 + \delta)} \tag{103}$$

Substituting in Equation (98) Equations (8), (15), (18), (96), (100), and (103) we obtain

$$B = \sqrt{(1 + \delta)}\left[\frac{\lambda^3(1 + \lambda)}{2}(1 + \delta) + \frac{1 + \lambda^3}{2\lambda}\right] - 2\lambda(1 + \delta) \tag{104}$$

If we take that

$$\sqrt{(1 + \delta)} = 1 + \frac{\delta}{2} - \frac{\delta^2}{8} + O(\delta^3) \tag{105}$$

we conclude that Equation (104) can be represented to $O(\delta^2)$ by

$$B = \delta^3 \frac{35\lambda^4(1+\lambda) - (1+\lambda^3)}{16\lambda}$$

$$+ \delta \frac{7\lambda^4(1+\lambda) + (1+\lambda^3) - 8\lambda^2}{4\lambda}$$

$$+ \frac{\lambda^4(1+\lambda) + (1+\lambda^3) - 4\lambda^2}{2\lambda} \qquad (106)$$

For $\lambda=1$ (the case of the spheroid) the same relation as Green's is obtained. From Equation (104) we can evaluate δ in terms of the Bond number and from Equations (101), (102), and (103) we have a_1, a_2, a_3 in terms of the radius of the sphere with equal volume. Thus, from Equations (84) and (85) we can evaluate the average cross-section and the average backscattering cross-section, respectively.

II.6. RANDOMLY ORIENTED ELLIPSOIDAL PARTICLES

In order to take into account the orientation of the scattering particles we will take the average depending on the orientation. Thus, we choose a reference rectangular Cartesian coordinate system (y_1, y_2, y_3) and introduce as unknown the Euler angles of the transformation (by rotation) from the reference system to one coinciding with the principal axes of the ellipsoid. For the unit vectors of the (y_1, y_2, y_3) system in terms of $\hat{\mathbf{x}}_i$ (the unit vectors of the sys-

tem which coincides with the principal axes of the ellipsoid) we have

$$\hat{\mathbf{y}} = \hat{\mathbf{x}} \cdot \tilde{D} \quad \text{for} \quad i = 1,2,3 \tag{107}$$

where the elements of the matrix $\tilde{D}$ are functions of the Euler angles and are given by the relations

$$d_{11} = \sin\theta_1 \sin\theta_2 + \cos\theta_1 \cos\theta_2 \cos\theta_3 \tag{108a}$$

$$d_{12} = \cos\theta_1 \sin\theta_2 - \sin\theta_1 \cos\theta_2 \cos\theta_3 \tag{108b}$$

$$d_{13} = \cos\theta_2 \sin\theta_3 \tag{108c}$$

$$d_{21} = \sin\theta_1 \cos\theta_2 + \cos\theta_1 \sin\theta_2 \cos\theta_3 \tag{108d}$$

$$d_{22} = \cos\theta_1 \cos\theta_2 + \sin\theta_1 \sin\theta_2 \cos\theta_3 \tag{108e}$$

$$d_{23} = - \sin\theta_2 \sin\theta_3 \tag{108f}$$

$$d_{31} = - \cos\theta_1 \sin\theta_3 \tag{108g}$$

$$d_{32} = \sin\theta_1 \sin\theta_3 \tag{108h}$$

$$d_{33} = \cos\theta_3 \tag{108i}$$

where $0 \leq \theta_i \leq \pi/2$ for $i=1,2,3$.

We mentioned before that the angle θ_3 is the angle between the y_3 and the x_3 axes. The x_1x_2 plane intersects the y_1y_2 plane in a line, which is called the nodal line. The q_1 angle is the angle between the nodal line and the y_1-axis and q_2 is the angle between the x_1-axis and the nodal line.

The relations between the components of the vectors relative to the reference frame and the frame coinciding with the principal axis of the ellipsoid are

$$k_m = \sum_{m=1}^{3} d_{jm} k_j' \qquad \text{for } m = 1,2,3 \tag{109}$$

$$b_m = \sum_{m=1}^{3} d_{jm} b_j' \qquad \text{for } m = 1,2,3 \tag{110}$$

where

$$\hat{\mathbf{k}} = \sum_{m=1}^{3} k_m \hat{\mathbf{x}}_m = \sum_{m=1}^{3} k_m' \hat{\mathbf{y}}_m' \tag{111}$$

$$\hat{\mathbf{b}} = \sum_{m=1}^{3} b_m \hat{\mathbf{x}}_m = \sum_{m=1}^{3} b_m' \hat{\mathbf{y}}_m' \tag{112}$$

So, in order to take the scattering cross-section and the radar cross-section over all the orientations we obtain

$$\langle\sigma\rangle = \int_0^{\pi/2}\int_0^{\pi/2}\int_0^{\pi/2} \sigma(\theta_1,\theta_2,\theta_3)\, f(\theta_1,\theta_2,\theta_3)\, d\theta_1 d\theta_2 d\theta_3 \qquad (113)$$

where $f(\theta_1,\theta_2,\theta_3)$ is the probability density function for the angles $(\theta_1,\theta_2,\theta_3)$ and $\sigma(\theta_1,\theta_2,\theta_3)$ is the scattering cross-section given by Equation (72) after the substitution of the components k_m, b_m in terms of k_m', b_m'.

Similarly for the backscattering cross-section we have the average over orientation

$$\langle\sigma_b\rangle = \int_0^{\pi/2}\int_0^{\pi/2}\int_0^{\pi/2} \sigma_b(\theta_1,\theta_2,\theta_3)\, f(\theta_1,\theta_2,\theta_3)\, d\theta_1 d\theta_2 d\theta_3 \qquad (114)$$

If we want to obtain the average over the size and orientation we must substitute in Equations (113) and (114) the terms σ and σ_b by the averages given by Equations (84) and (85), respectively.

II.7. NUMERICAL RESULTS - DISCUSSION

The solutions presented in the above sections can be tested numerically against the known solutions for their special cases. For example, if $a_1=a_2=a_3$ we can use the solution of Rayleigh [8]. Figure 2 in the Appendix A presents both solution and the differences are indistinguishable. Another

spectial case of interest in radar-rainfall estimation is that of an oblate spheroid. Plots in Appendix A present the comparison with the Gans' solution for both single scatterer and volume scattering cases. Computer programs written in FORTRAN are included in Appendix B.

II.8. FURTHER RESEARCH

In the present work we have examined the scattering of raindrops in the Rayleigh region. We have assumed the shape of the large drops as an ellipsoidal one and we have calculated the Rayleigh approximation up to the first order. In order to improve the accuracy of our results we have to take into account the second order approximation of the Rayleigh series as well. Further, for the particle size distribution, when we calculate the sum of the curvature, at any point of the ellipsoid, we have to assume a more "realistic" average value of the sum of the curvatures.

In order to derive numerical results taking into account the random orientation of the raindrops as well, we have to think about the probability density function, for the Euler angles. Beard and Jameson's results about the canting of the raindrops give us enough information for the probability density function for one of the three Euler angles [9].

If we want to have more accuracy for the scattering problem of the large raindrops, we have to assume that their shape is better approximated by a spherical cap. The only known results for spherical caps are due to Thomas [40] for the acoustical case and to Collins [14,15] for the electromagnetic case. These last results have been obtained assuming different boundary conditions from that which we consider on the raindrop surface. From a mathematical point of view

such a study would be rather difficult, but the results would be applicable for the entire range of frequencies.

The consideration of the scattering of the raindrops as a multi-scattering problem is also another possibility. Such an investigation can be based on Twersky's work [41]. We also can examine the possibility of exploiting the results of Peterson and Ström [33] who have generalized the T-matrix approach of Waterman for the case of multiple scattering by N arbitrarily shaped configurations.

II.5. REFERENCES

1. Angell, T.S. and Kleinman, R.E., "Polarizability tensor in low-frequency inverse scattering," Radio Science, V. 22, No. 7, p. 1120 (1987).
2. Asano, S. and Yamamoto, G., "Light scattering by a spheroidal particle," Applied Optics, V. 14, No. 2, p. 29 (1975).
3. Asano, S., "Light scattering properties of spheroidal particles," Applied Optics, V. 18, No. 5, p. 712 (1979).
4. Asano, S. and Sato, M., "Light scattering by randomly oriented spheroidal particles," Applied Optics, V. 19, No. 6, p. 962 (1980).
5. Asvestas, J. and Kleinman, R., "Low frequency scattering by spheroids and disks. 1. Dirichlet Problem for a Prolate spheroid," J. Inst. Maths. Applics., V. 6, p. 42 (1969).
6. Asvestas, J. and Kleinman, R., "Low frequency scattering by spheroids and disks. 2. Neumann problem for a prolate spheroid," J. Inst. Maths. Applics., V. 6, p. 57 (1969).
7. Barber, P. and Yeh, C., "Scattering of electromagnetic waves by arbitrarily shaped dielectric bodies," Applied Optics, V. 14, No. 12, p. 2869 (1975).
8. Battan, L.J., "Radar observation of the atmosphere," Un. of Chicago Press (1981).
9. Beard, K.V. and Jameson, A.R., "Raindrop canting," J. Atmosph. Sci., V. 40, p. 448 (1983)

10. Beard, K.V., Feng, J.Q., and Chuang, C.C., "A simple perturbation model for the electrostatic shape of falling drops," J. Atmosph. Sci., V. 46, No. 15, p. 2404 (1989).

11. Boren, C.F. and Huffman, D.R., "Absorption and scattering of light by small particles," Wiley-Interscience (1983).

12. Bohren, C.F. and Singham, S.B., "Backscattering by nonspherical particles: A review of methods; Suggested new approaches," (to appear).

13. Chuang, C.C. and Beard, K.V., "A numerical model for the equilibrium shape of electrified raindrops," Am. Met. Society (1990).

14. Collins, W.D., " Some scalar diffraction problems for a spherical cap," Arch. Rat. Mech. Anal., Vol. 10, p. 249 (1962).

15. Collins, W.D., "Note on the electrified spherical cap," Proc. Camb. Phil. Soc., V. 55, p. 377 (1959).

16. Darling, D.A. and Senior, T.B.A., "Low-frequency expansions for scattering by separable and nonseparable bodies," J. Acoust. Soc., V. 37, No. 2, p. 228 (1963).

17. Dassios, G., "Convergent low-frequency expansions for penetrable scatterers," Doct. Dis., Univ. IllinoisChicago Circle (1975).

18. Green, A.W., "An approximation for the shape of large raindrops," J. Appl. Meteor., V. 14, p. 1578 (1975).

19. Hobson, W., "The theory of spherical and ellipsoidal harmonics," Chelsey (1953).

20. Ishimaru, A., ":Wave propagation and scattering in random media," Academic press (1978).

21. Jameson, A.R., "Microphysical interpretation of multi-parameter radar measurements in rain. Part I: Interpretation of polarization measurements and estimation of raindrop shapes," J. Atmos. Sci., V. 40, No. 7, p. 1792 (1983).

22. Jameson, A.R., "Microphysical interpretation of multi-parameter radar measurements in rain. Part II: Estimation of raindrop distribution parameters by combined dual-wavelength and polarization measurements," J. Atmos. Sci., V. 40, No. 7, p. 1803 (1983).

23. Jameson, A.R., "A comparison of microwave techniques for measuring rainfall (to be published).

24. Jackson, J.D., "Classical electrodynamics," J. Wiley (1975).

25. Jones, D.S., "The scattering of long electromagnetic waves," Q.J. Mech. Appl. Math., Vol. 33, p. 1 (1980).

26. Jones, D.S., "Acoustic and electromagnetic waves," Oxford Sc. Publ. (1978).

27. Kerker, M., "The scattering of light and other electromagnetic radiation," Academic, N. York (1969).

28. Kiriaki, K. and Athanassiadis, C., "Low frequency electromagnetic scattering theory for a dielectric," Bul. Greek Math. Soc., V. 27, p. 47 (1986).

29. Kleinman, R.E. "Low-frequency solution of electromagnetic scattering problems," Delft Symposium, p. 891 Pergamon (1967).

30. Kleinman, R.E. and Senior, T.B.A., "Rayleigh scattering cross-sections," Radio Science, Vol. 7, No. 10, p. 937 (1972).

31. Moon, P. and Spencer, D.E., "Field theory handbook, Springer-Verlag (1971).

32. Morse, P.M. and Feshbach, H., "Methods of theoretical physics," McGraw-Hill (1953).

33. Peterson, B. and Ström, St., "T-Matrix for electromagnetic scattering from an arbitrary number of scatterers and representations of E(3)*," Phy. Review D., Vol. 8, No. 10, p. 3361 (1973).

34. Pruppacher, H.R. and Klett, J.D., "Microphysics and clouds and precipitation," Reidel Publ. Company (1980).

35. Rayleigh, J.W.S., "On the incidence of aerial and electrical waves upon small obstacles in the form of ellipsoids or elliptic cylinders and on the passage of electric waves through a circular aperture in a conducting screen," Phil. Mag. 44, p. 28 (1897).

36. Seigel, K.M., "For field scattering from bodies of revolution," Appl. Sci. Res., Section B, V. 7, p. 293 (1959).

37. Stevenson, A.F., "Solution of electromagnetic scattering problems as power series in the ratio (dimension of scatterer)/wavelength," J. Appl. Phys. 24, p. 1134 (1953).

38. Stevenson, A.F., "Electromagnetic Scattering by an Ellipsoid in the Third Approximation," J. Appl. Phys. 24, p. 1143 (1953).

39. Stratton, J.A., "Electromagnetic theory," McGraw-Hill (1941).

40. Thomas, D.P., "Diffraction by a spherical cap," Proc. Camb. Phil. Soc., Vol. 59, p. 197 (1963)

41. Twersky, V., "Multiple scattering of electromagnetic waves by arbitrary configurations," J. Math. Phys. 8, p. 589 (1967).

42. Ulbrich, C.W., "A review of the differential reflectivity technique of measuring rainfall," IEEE Trans. of Geosc. and Remote Sensing, V. GE24, No. 6, p. 955 (1986).

43. Van de Hulst, H.C., "Light scattering by small particles," Wiley, N. York (1957).

44. Warner, C. and Hizal, A., "Scattering and depolarization of microwaves by spheroidal raindrops," Radio Science, V. 11, No. 11, p. 921 (1976).

45. Waterman, C.P., "Symmetry, Unitarity, and Geometry in Electromagnetic Scattering," Phys. Review D, V. 3, No. 4, p. 825 (1971).

46. Doviak, R.J. and D.S. Zrnic, "Doppler Radar and Weather Observations", Academic Press, 1984.

APPENDIX A - PLOTS

SCATTERING FROM WATER SPHERES

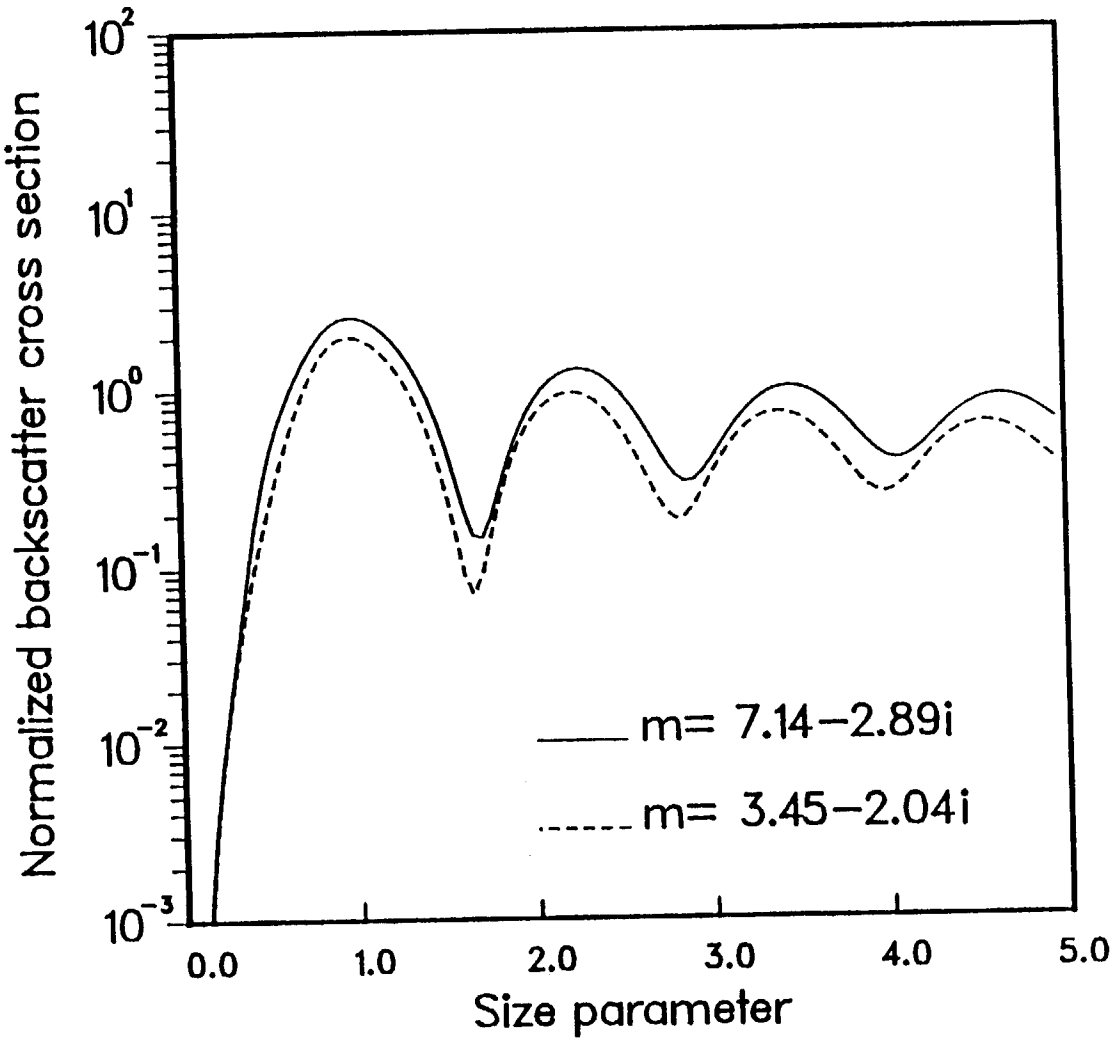

SCATTERING FROM WATER SPHERES

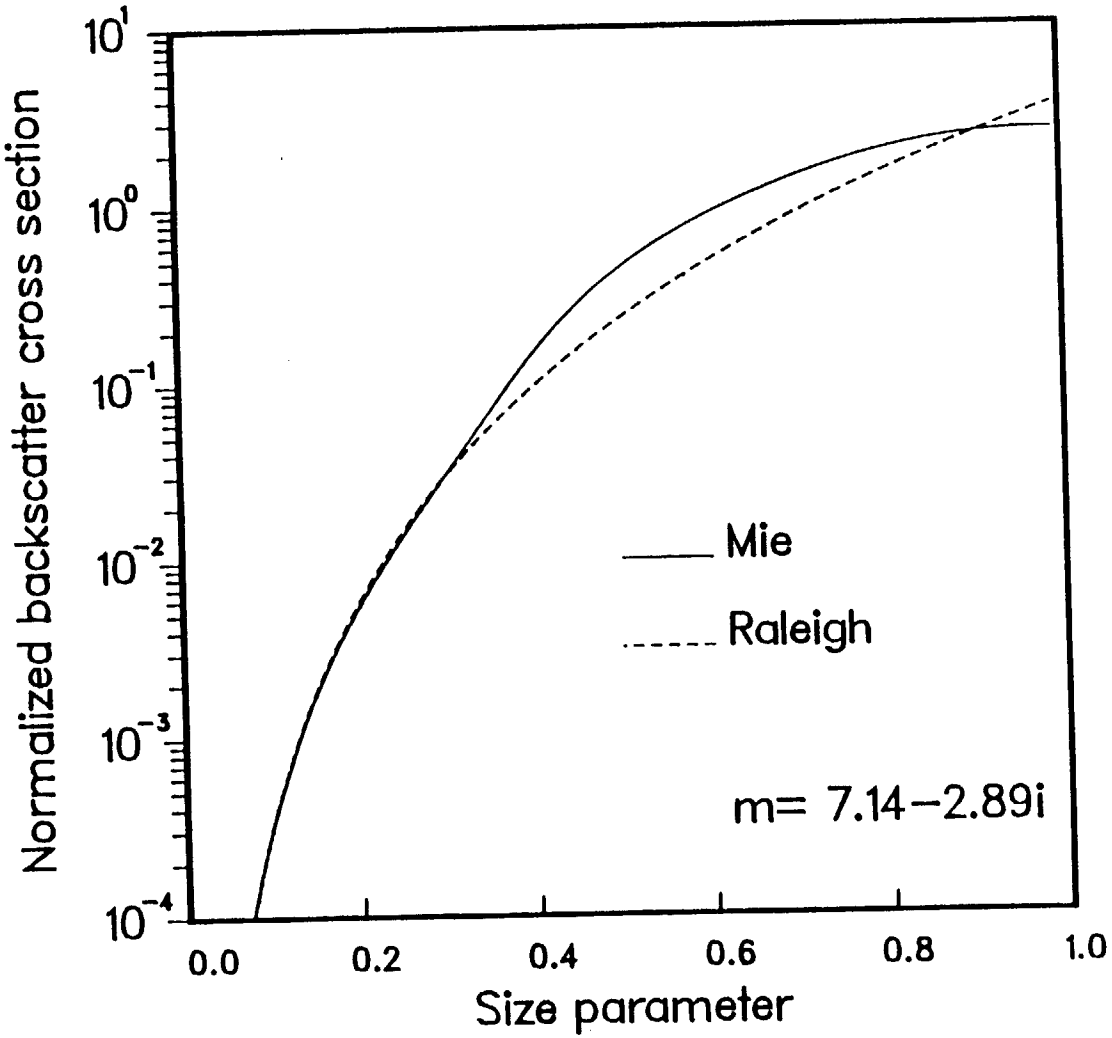

SCATTERING FROM WATER SPHERES

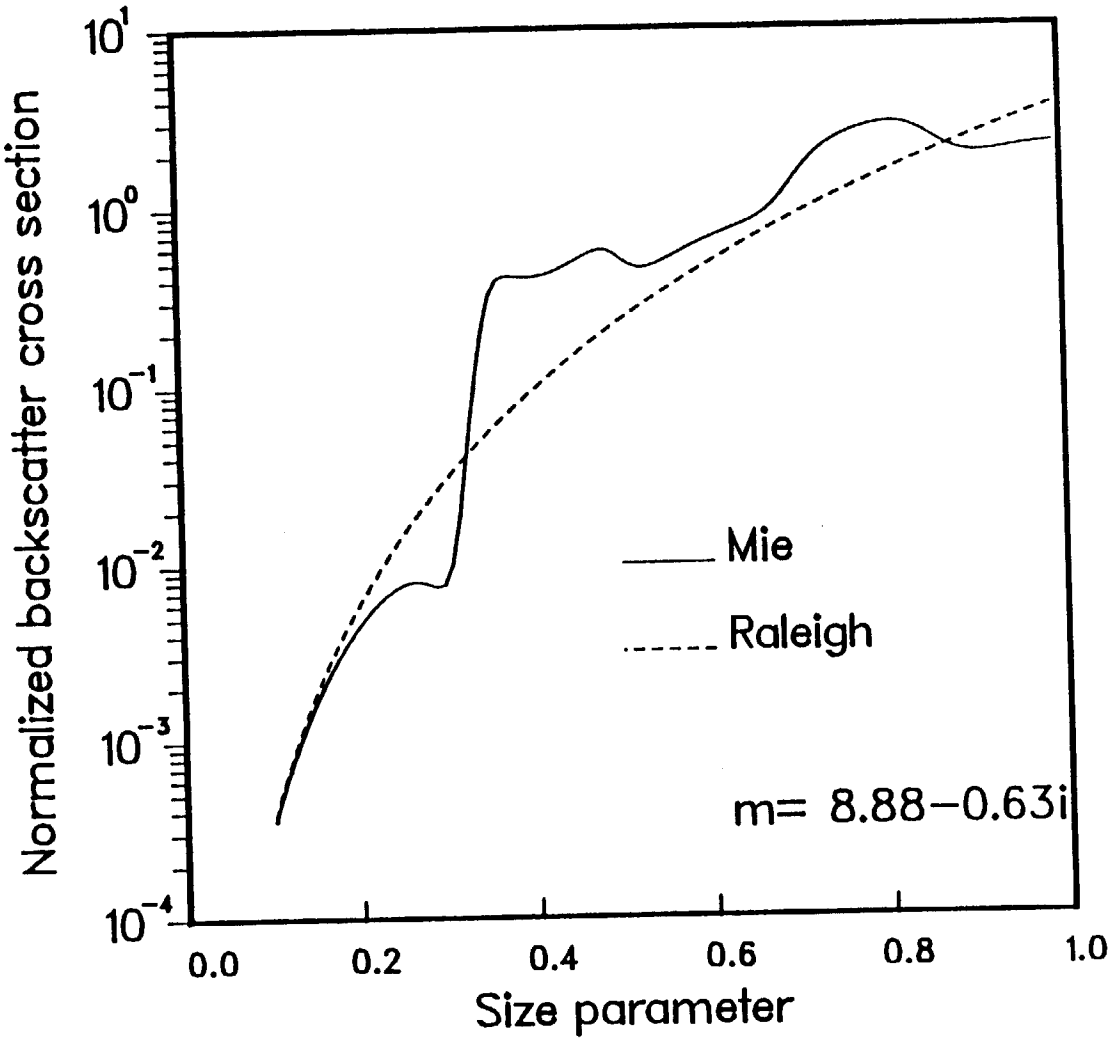

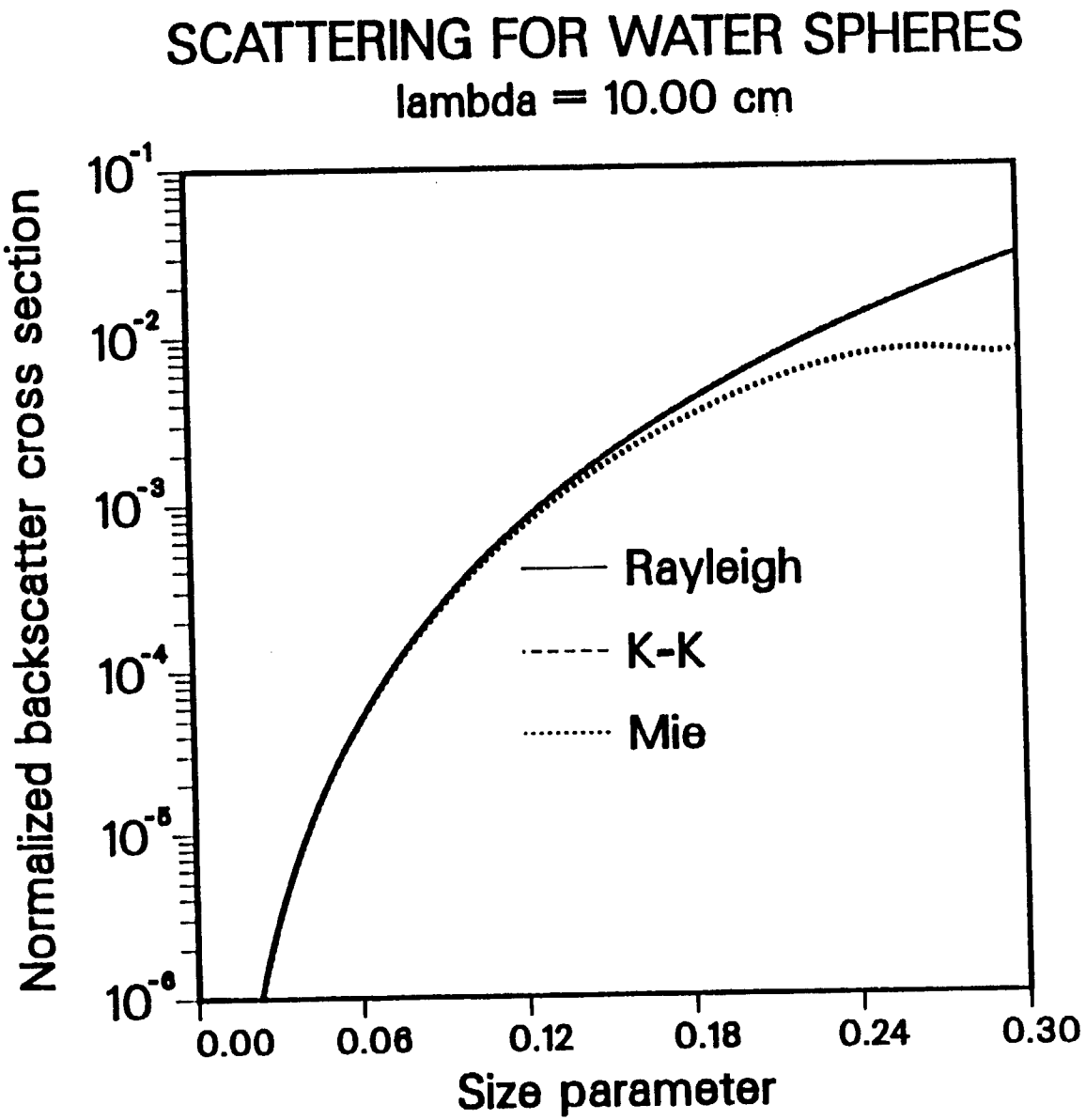
SCATTERING FOR WATER SPHERES
lambda = 10.00 cm
Normalized backscatter cross section
10^{-1}
10^{-2}
10^{-3}
10^{-4}
10^{-5}
10^{-6}
Rayleigh
K-K
Mie
0.00
0.06
0.12
0.18
0.24
0.30
Size parameter

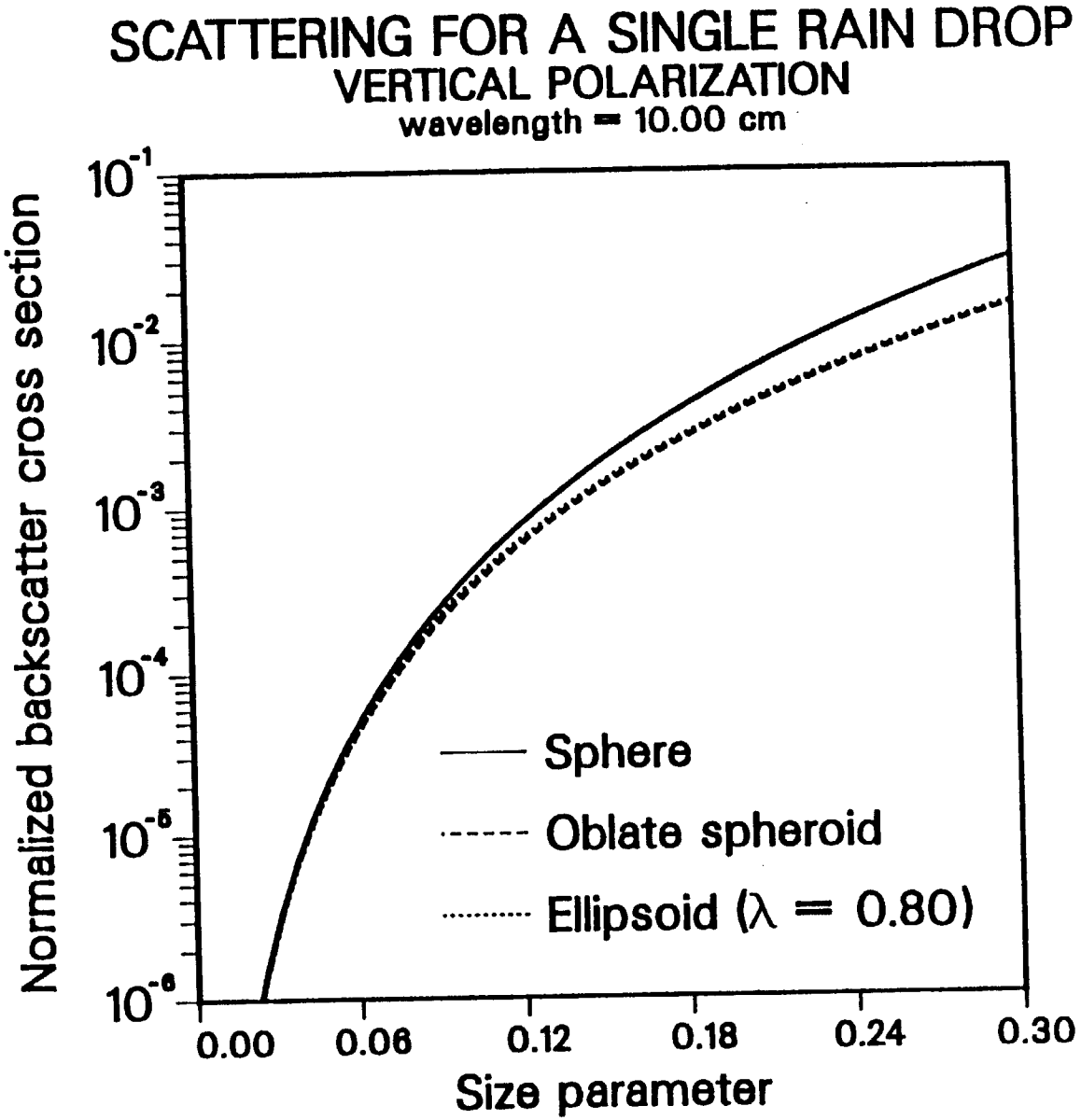
SCATTERING FOR A SINGLE RAIN DROP
VERTICAL POLARIZATION
wavelength = 10.00 cm
Normalized backscatter cross section
10^{-1}
10^{-2}
10^{-3}
10^{-4}
10^{-5}
10^{-6}
Sphere
Oblate spheroid
Ellipsoid (λ = 0.80)
0.00
0.06
0.12
0.18
0.24
0.30
Size parameter

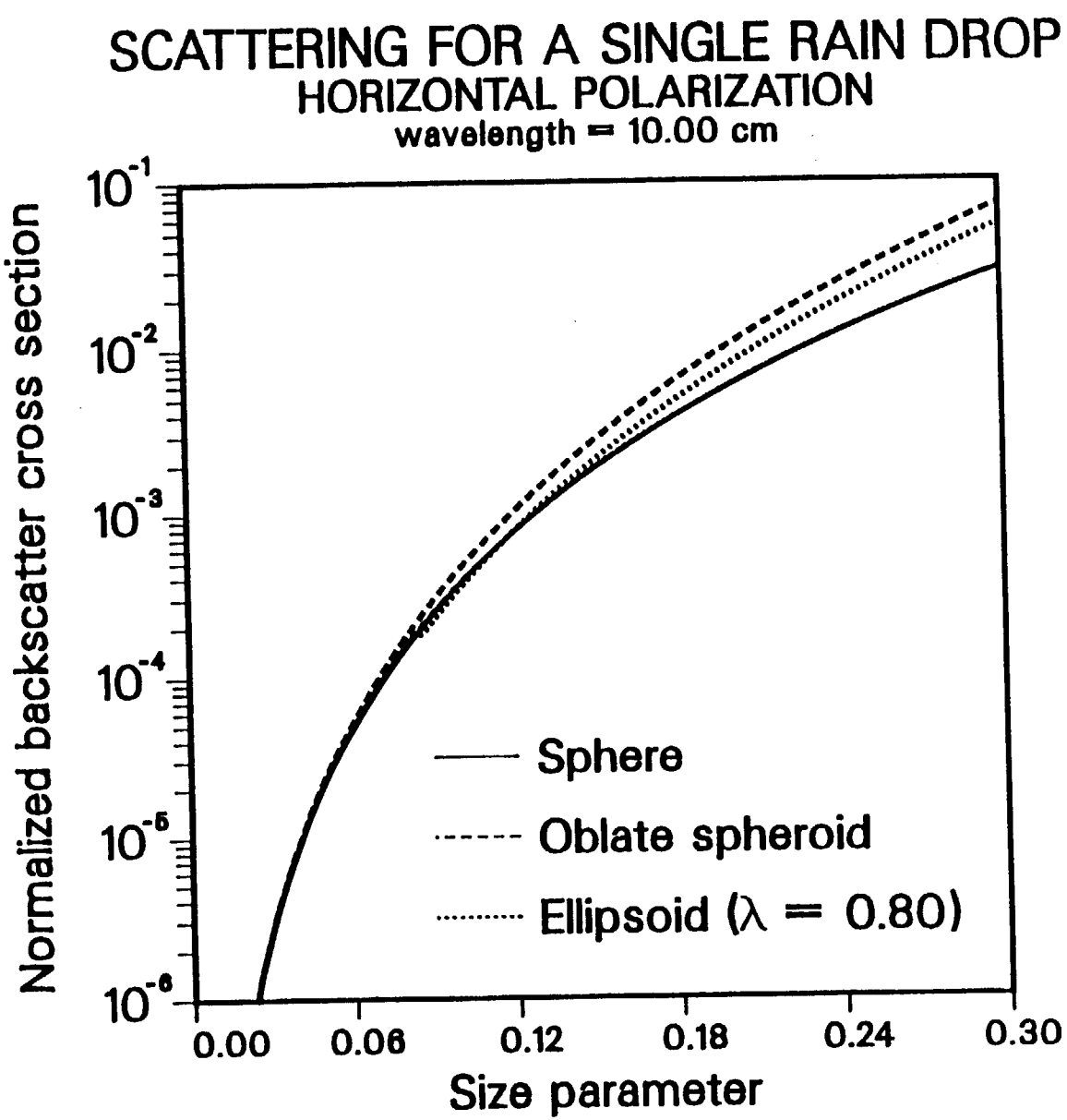
SCATTERING FOR A SINGLE RAIN DROP
HORIZONTAL POLARIZATION
wavelength = 10.00 cm
Normalized backscatter cross section
10^{-1}
10^{-2}
10^{-3}
10^{-4}
10^{-5}
10^{-6}
0.00
0.06
0.12
0.18
0.24
0.30
Size parameter
Sphere
Oblate spheroid
Ellipsoid (λ = 0.80)

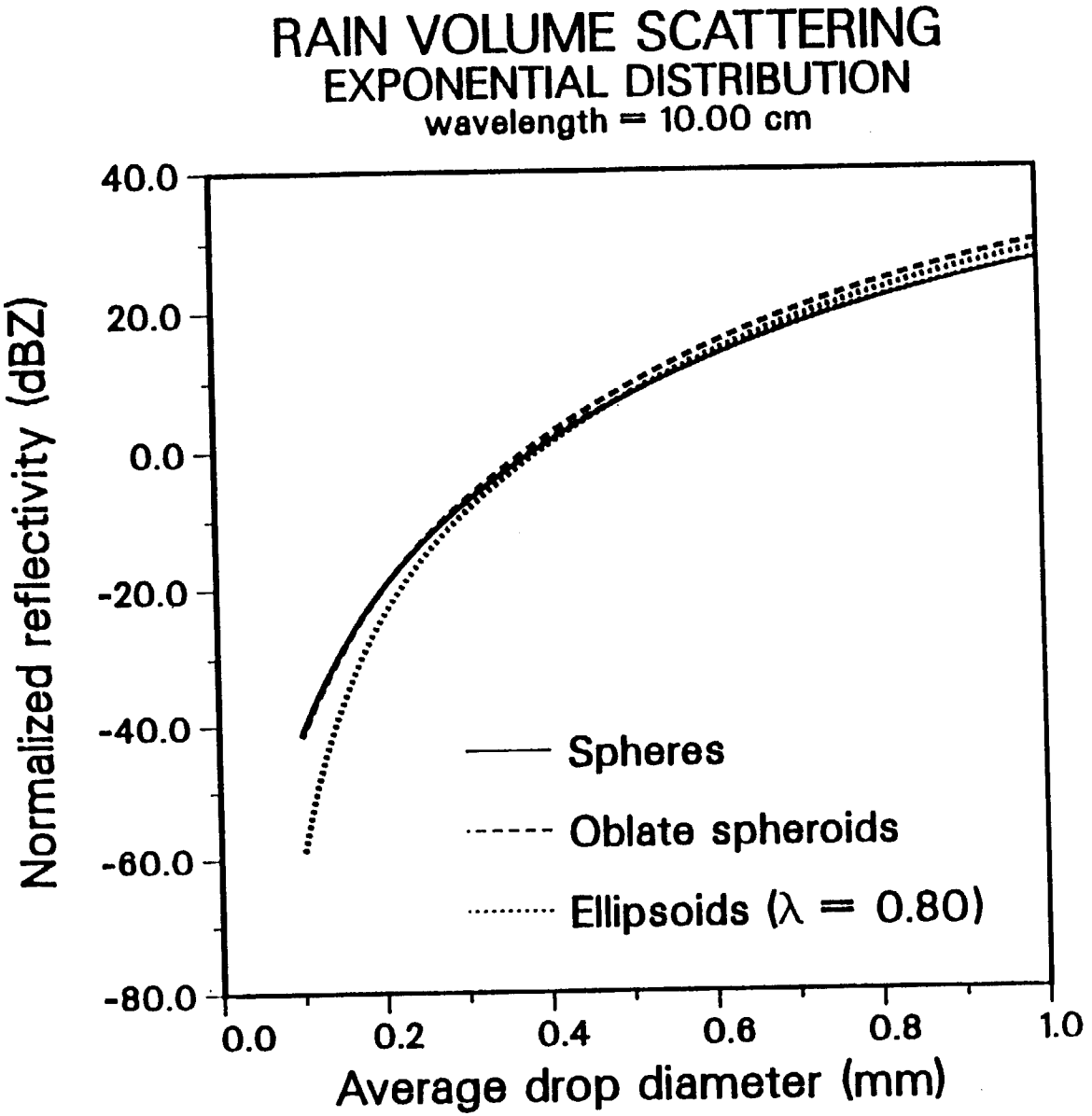
RAIN VOLUME SCATTERING
EXPONENTIAL DISTRIBUTION
wavelength = 10.00 cm
Normalized reflectivity (dBZ)
40.0
20.0
0.0
-20.0
-40.0
-60.0
-80.0
0.0
0.2
0.4
0.6
0.8
1.0
Average drop diameter (mm)
Spheres
Oblate spheroids
Ellipsoids (λ = 0.80)

APPENDIX B - PROGRAMS

```
c*    ****************************************************************
      subroutine kuli(am,rk,bm,rmag_sus,eps1,eps2,rlambda,sigmab)
c*    ****************************************************************
c*
c*
c*    *** subroutine calculates the radar cross-section for an
c*        ellipsoidal scatterer (Kiriaki-Krajewski method)
c*        (uses IMSL special functions)
c*
c           Parameters:
c               am        - vector of ellipsoid axes (m)
c               rk        - unit vector of incident wave direction
c               bm        - unit vector of polarization
c               rmag_sus  - magnetic suseptibility of the scatterer
c               eps1      - dialectric constant for the scatterer
c               eps2      - dielectric constant for the medium
c               rlambda   - wavelength (m)
c               sigmab    - backscattering crossection (output, m**2)
c
      implicit real*8(A-H,O-Z)
      dimension A(3),am(3),B(3),rk(3),bm(3),RI1(3),h(3)
c*
      pi=DCONST('PI')
      constant=4.*pi/9.
      wave_num=2.0*pi/rlambda
c*
      x=am(1)*am(1)
      y=am(2)*am(2)
      z=am(3)*am(3)
      a123=am(1)*am(2)*am(3)
c*
      h(1)=sqrt(y-z)
      h(2)=sqrt(x-z)
      h(3)=sqrt(x-y)
c*
      sss=DMACH(1)
      bbb=DMACH(2)
c*
      RI1(1)=DELRD(y,z,x)/3.0
      RI1(2)=DELRD(x,z,y)/3.0
      RI1(3)=DELRD(x,y,z)/3.0
c*
      sum=RI1(1)+RI1(2)+RI1(3)
      zp=1.0/(am(1)*am(2)*am(3))
c*
      coeff1=eps2/eps1 -1.
      coeff2=4.0*pi*rmag_sus
      coeff3=a123*coeff2
c*
```

```
      do m=1,3
        ar=bm(m)*coeff1
        A(m)=ar/(a123*coeff1*RI1(m)+1.)
      enddo
c*
      B(1)=coeff2*(rk(2)*bm(3)-rk(3)*bm(2))
     *     /(coeff3*RI1(1)+1.)
      B(2)=coeff2*(rk(3)*bm(1)-rk(1)*bm(3))
     *     /(coeff3*RI1(2)+1.)
      B(3)=coeff2*(rk(1)*bm(2)-rk(2)*bm(1))
     *     /(coeff3*RI1(3)+1.)
c*
      sum=0.0
c*
      do i=1,3
        sum=sum+A(i)*rk(i)
      enddo
c*
      s1=(A(1)-rk(1)*sa+rk(3)*B(2)-rk(2)*B(3))**2
      s2=(A(2)-rk(2)*sa+rk(1)*B(3)-rk(3)*B(1))**2
      s3=(A(3)-rk(3)*sa-rk(2)*B(1)-rk(1)*B(2))**2
c*
      zp=x*y*z
      sigmab=wave_num**4*constant*zp*(s1+s2+s3)
c*
      return
      end
```

```
c*    ****************************************************************
      subroutine rayleigh(crindx,alfa,sigma)
c*    ****************************************************************
      COMPLEX crindx
c*
C*    *** SUBROUTINE COMPUTES THE NORMALIZED CROSS SECTION FOR
C*        A SPHERE IN RALEIGH SCATTERING REGIME
C*
      complex zp,K
c*
      zp=crindx*crindx
      K=(zp-1.0)/(zp+2.0)
      RK2=ABS(K)*ABS(K)
c*
      sigma=4.0*alfa**4*RK2
c*
      return
      end
```

```
C     ************************************************************
      subroutine bhmie(crindx,alfa,qext,qsca,qback)
C     ************************************************************
      complex crindx
c
c     *** Subroutine calculates Mie scattering by water spheres.
c         It is based on the program included in Bohren & Hoffman (1983
c
c         Parameters:
c             crindx - complex refractive index (relative)
c                      of the scatterer
c             alfa   - the size parameter (p*pi*radius/wavelength)
c             qext   - total extinction efficiency
c             qsca   - total scatering efficiency
c             qback  - normalized backscattering crossection
c
      dimension amu(100),theta(100),pai(100),tau(100),pi0(100),pi1(100)
      complex d(3000),y,xi,xi0,xi1,an,bn,s1(200),s2(200)
      double precision psi0,psi1,psi,dn,dx
c
      pi=CONST('PI')
      dx=alfa
      y=alfa*crindx
c
c     *** series terminated after nstop terms
c
      nang=11
      xstop=alfa+4.*alfa**0.3333+2.0
      nstop=xstop
      ymod=cabs(y)
      nmx=amax1(xstop,ymod)+15
      dang=pi/2./float(nang-1)
c
      do 100 j=1,nang
        theta(j)=(float(j)-1.)*dang
        amu(j)=cos(theta(j))
  100 continue
c
c     *** logarithmic derivative d(j) calculated by downward
c         recurrence beginning at j=nmx
c
      d(nmx)=cmplx(0.0,0.0)
      nn=nmx-1
c
      do 110 n=1,nn
        rn=nmx-n+1
        d(nmx-n)=(rn/y)-(1./(d(nmx-n+1)+rn/y))
  110 continue
c
```

```
      do 120 j=1,nang
        pi0(j)=0.0
        pi1(j)=1.0
  120 continue
c
      nn=2*nang-1
c
      do 130 j=1,nn
        s1(j)=cmplx(0.0,0.0)
        s2(j)=cmplx(0.0,0.0)
  130 continue
c
c     *** Riccati-Bessel functions with real argument x
c         calculated by upward recurrence
c
      psi0=dcos(dx)
      psi1=dsin(dx)
      chi0=-sin(alfa)
      chi1=cos(alfa)
      apsi0=psi0
      apsi1=psi1
      xi0=cmplx(apsi0,-chi0)
      xi1=cmplx(apsi1,-chi1)
      qsca=0.0
      n=1
c
  135 continue
      dn=n
      rn=n
      fn=(2.*rn+1.)/(rn*(rn+1.))
      psi=(2.*dn-1.)*psi1/dx-psi0
      apsi=psi
      chi=(2.*rn-1.)*chi1/alfa-chi0
      xi=cmplx(apsi,-chi)
c
      an=(d(n)/crindx+rn/alfa)*apsi-apsi1
      an=an/((d(n)/crindx+rn/alfa)*xi-xi1)
      bn=(crindx*d(n)+rn/alfa)*apsi-apsi1
      bn=bn/((crindx*d(n)+rn/alfa)*xi-xi1)
c
      qsca=qsca+(2.*rn+1.)*(cabs(an)*cabs(an)+cabs(bn)*cabs(bn))
c
```

```
      do 140 j=1,nang
        jj=2*nang-j
        pai(j)=pi1(j)
        tau(j)=rn*amu(j)*pai(j)-(rn+1.)*pi0(j)
        p=(-1.)**(n-1)
        s1(j)=s1(j)+fn*(an*pai(j)+bn*tau(j))
        t=(-1.)**n
        s2(j)=s2(j)+fn*(an*tau(j)+bn*pai(j))
        if(j.eq.jj) go to 140
        s1(jj)=s1(jj)+fn*(an*pai(j)*p+bn*tau(j)*t)
        s2(jj)=s2(jj)+fn*(an*tau(j)*t+bn*pai(j)*p)
  140 continue
c
      psi0=psi1
      psi1=psi
      apsi1=psi1
      chi0=chi1
      chi1=chi
      xi1=cmplx(apsi1,-chi1)
      n=n+1
      rn=n
c
      do 150 j=1,nang
        pi1(j)=((2.*rn-1.)/(rn-1.))*amu(j)*pai(j)
        pi1(j)=pi1(j)-rn*pi0(j)/(rn-1.)
        pi0(j)=pai(j)
  150 continue
c
      if (n-1-nstop.lt.0)then
        go to 135
      else
        qsca=(2./(alfa*alfa))*qsca
        qext=(4./(alfa*alfa))*real(s1(1))
        qback=(4./(alfa*alfa))*cabs(s1(2*nang-1))*cabs(s1(2*nang-1))
      endif
c
      return
      end
```

APPENDIX C - BIAS SIMULATION STUDY